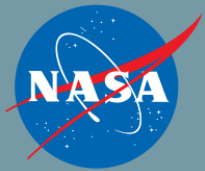


14th International Symposium on Nondestructive
Characterization of Materials
June 22 – 26, 2015

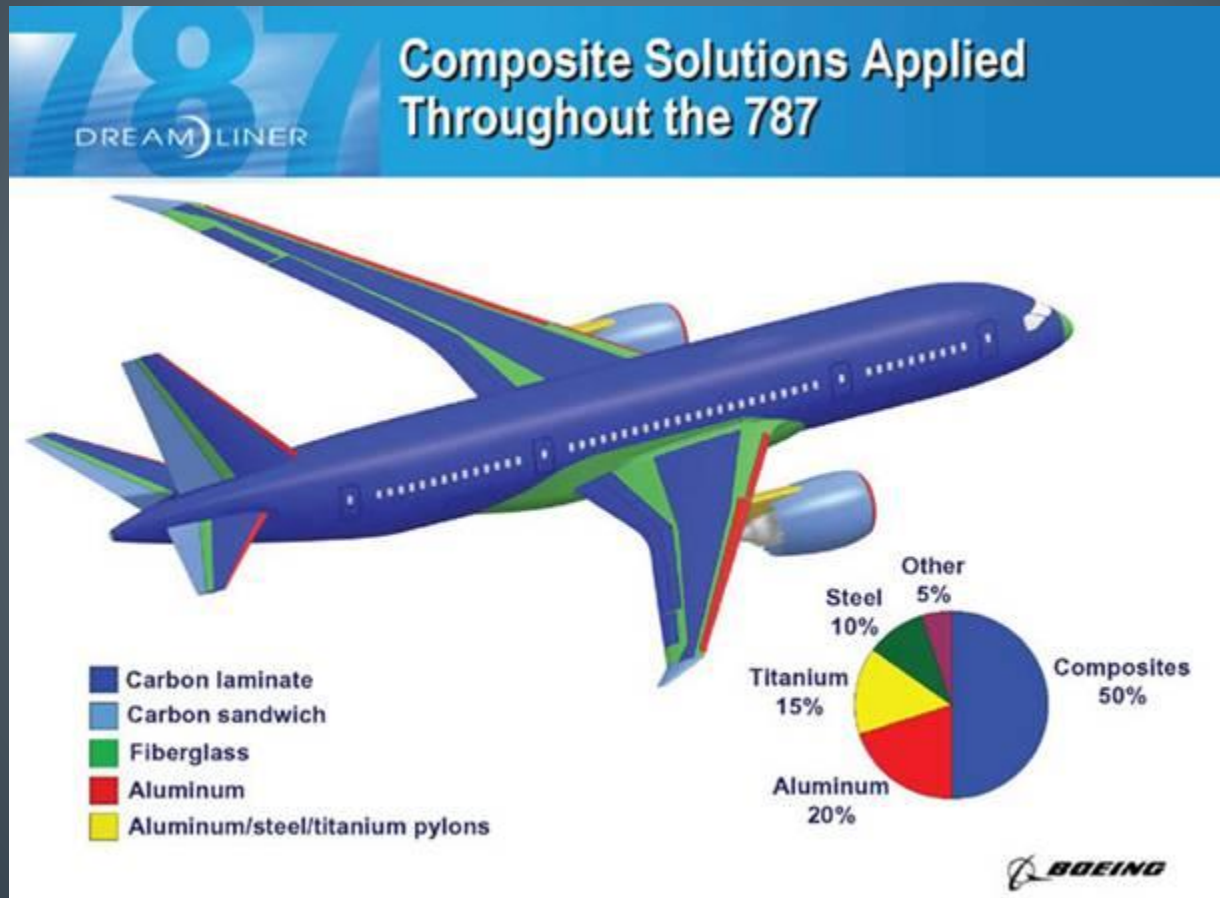
Composite characterization using laser Doppler vibrometry and multi- frequency wavenumber analysis

By Peter Juarez and Dr. Cara Leckey

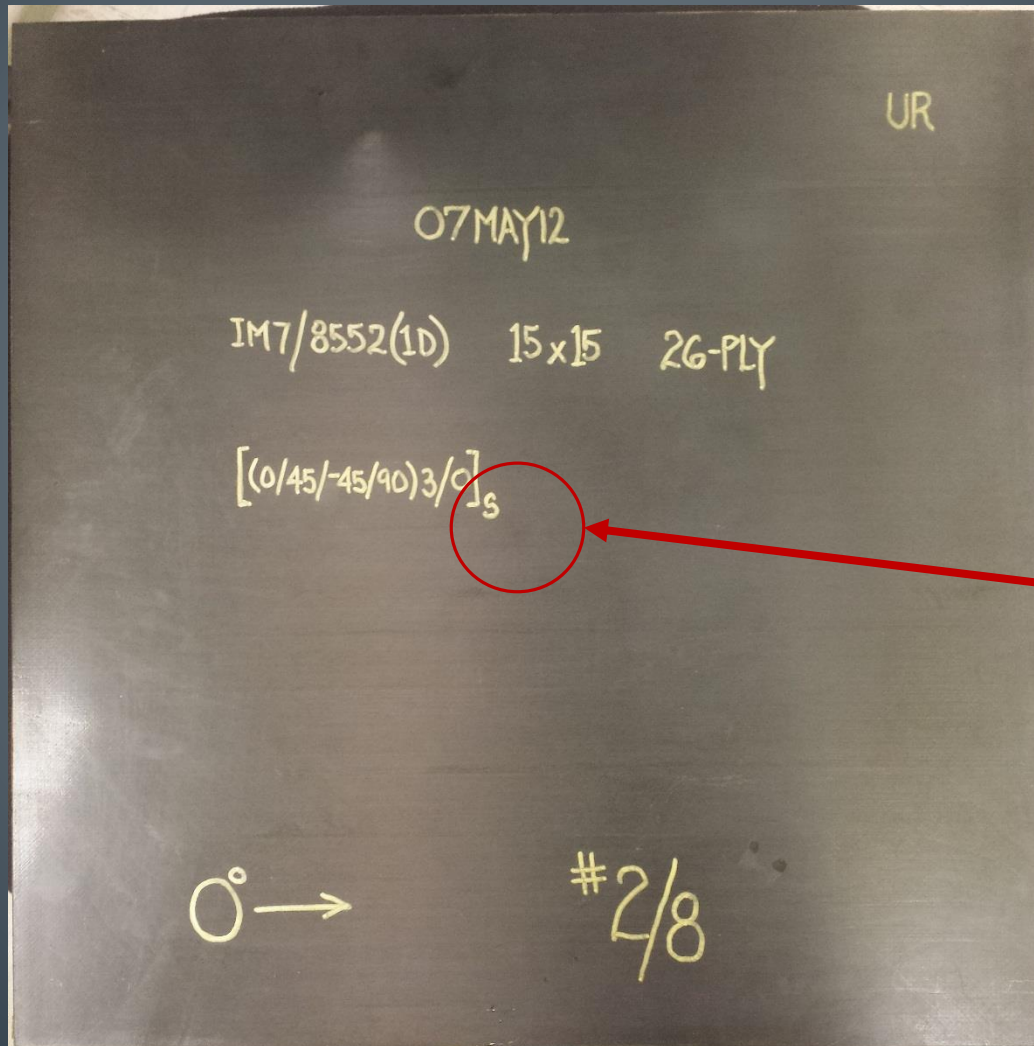


NASA Langley Research Center
Nondestructive Evaluation Sciences Branch

Motivation



Motivation

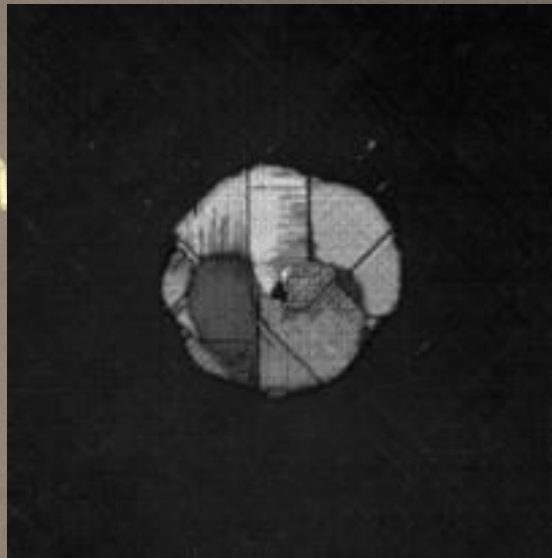


Barely Visible
Damage
(BVD)

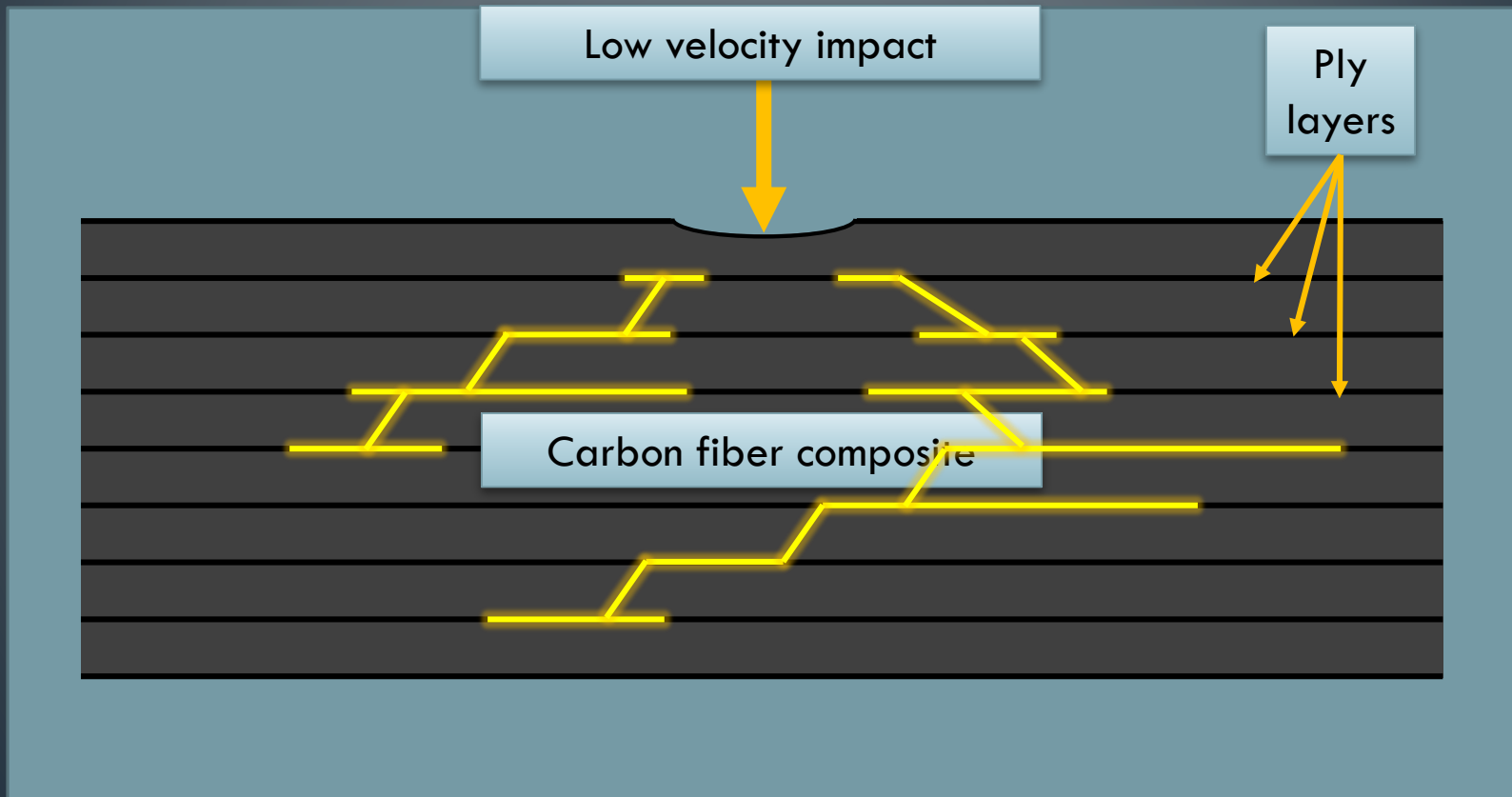
07 MAY 12

IM7/8552(1D) 15x15 2G-PLY

[(0/45/-45/9



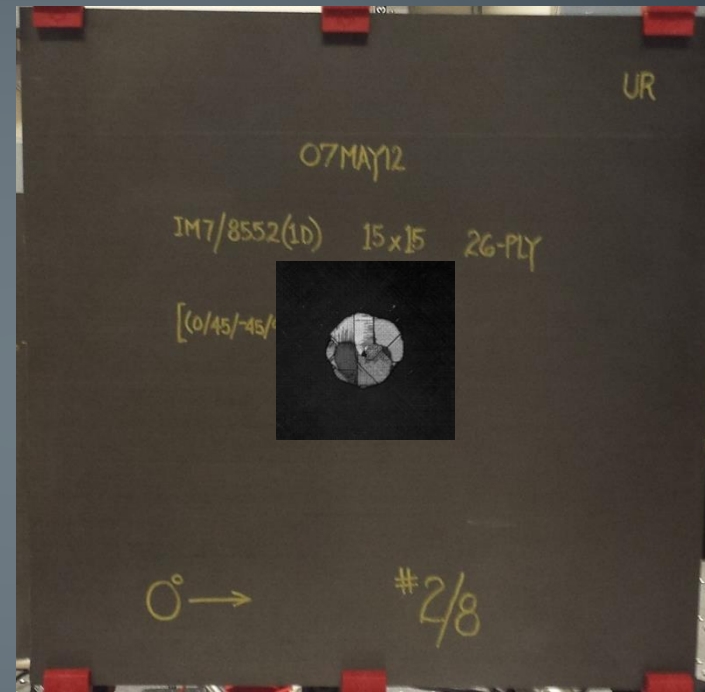
Motivation

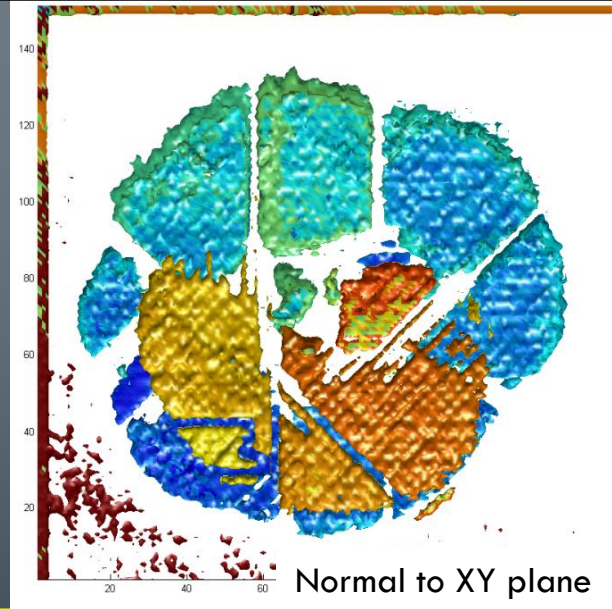
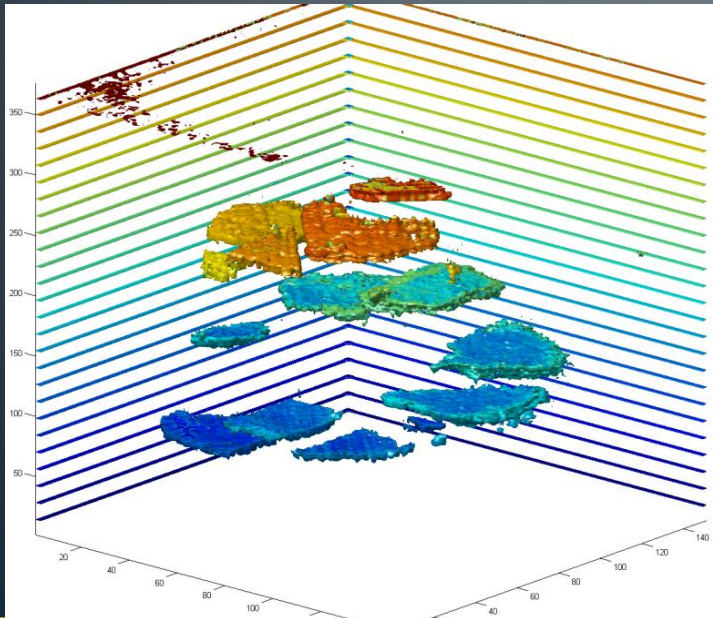
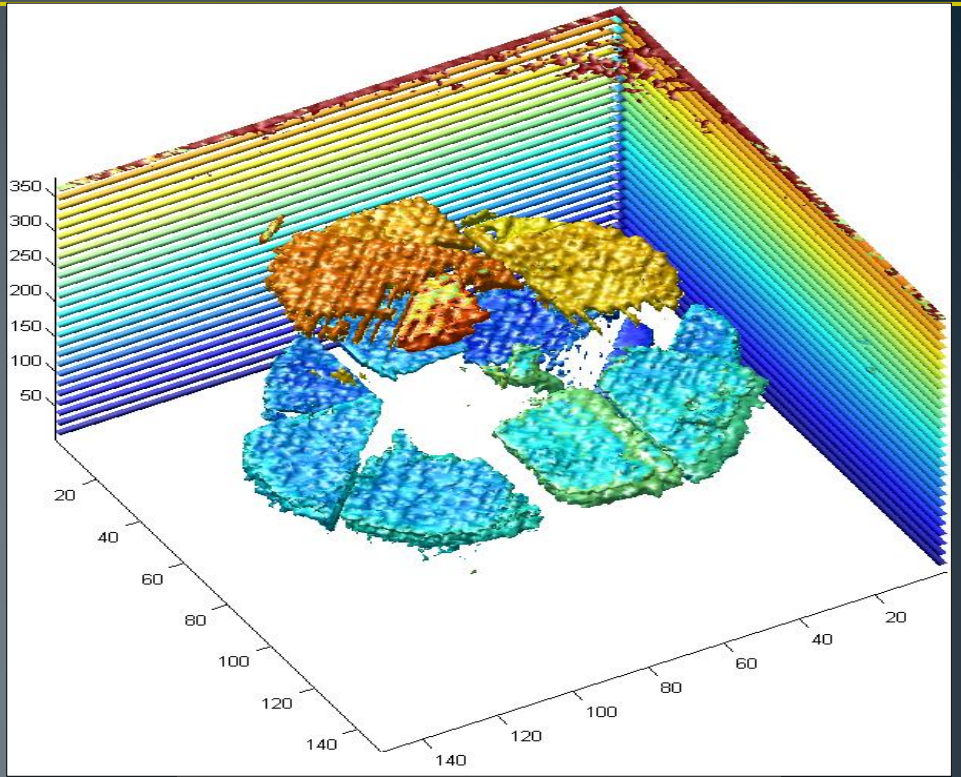
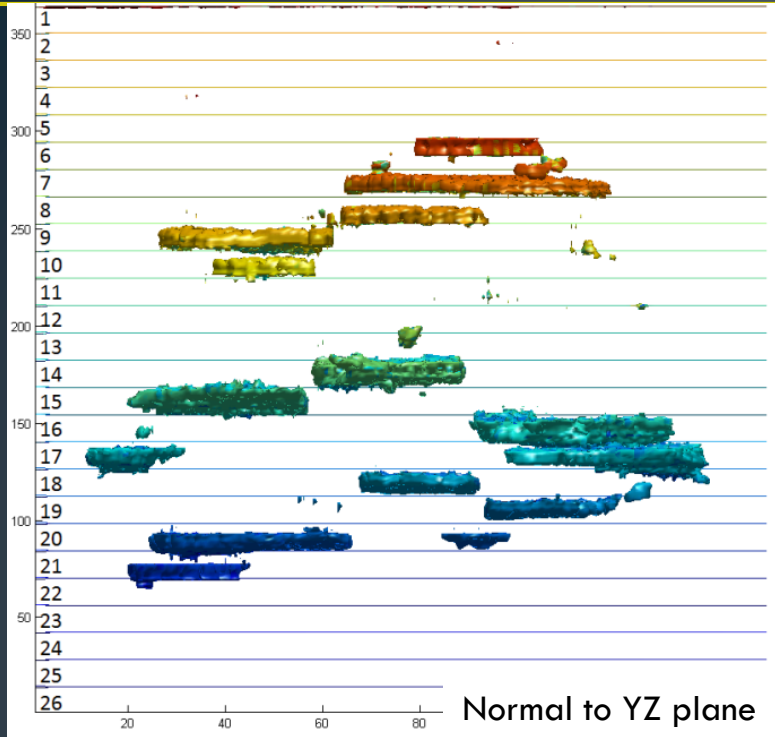


Goal of research



- 26 ply carbon fiber panel 15"x15", quasi-isotropic layup $([0/45/-45/90]_3/0)_s$
- Damaged using a static point load of 1511 lbf until failure, then scanned using a traditional nondestructive evaluation technique (ultrasonic immersion tank scanning)

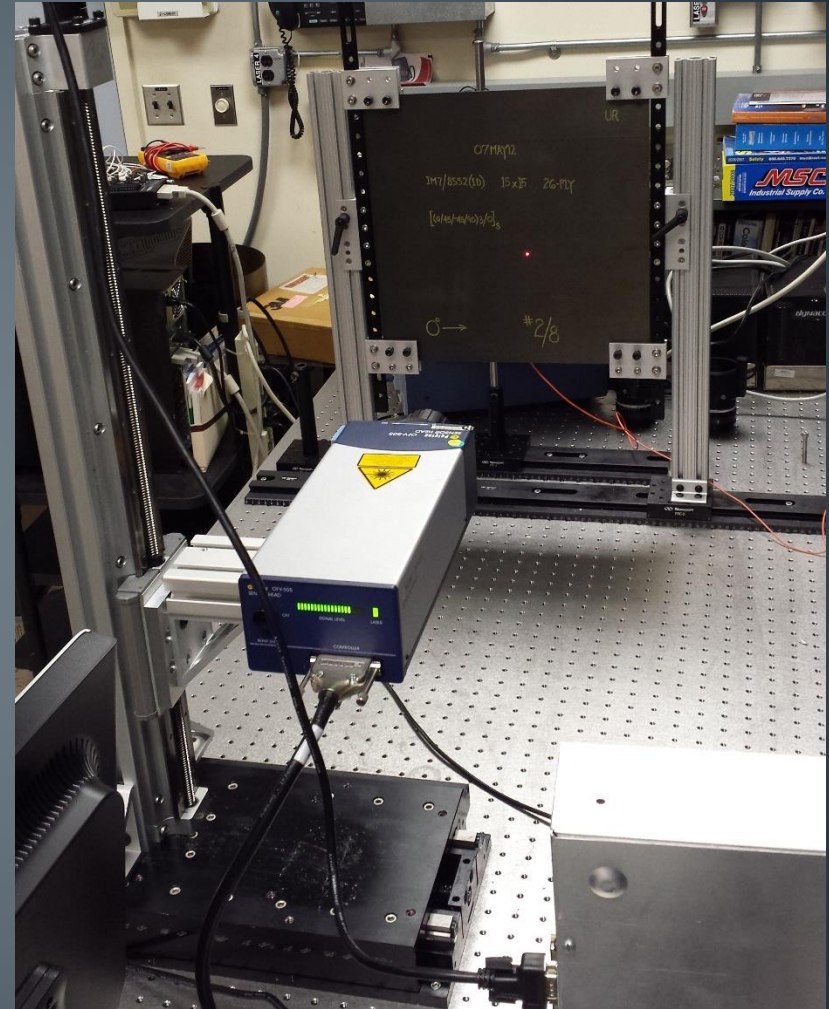




Goal of research

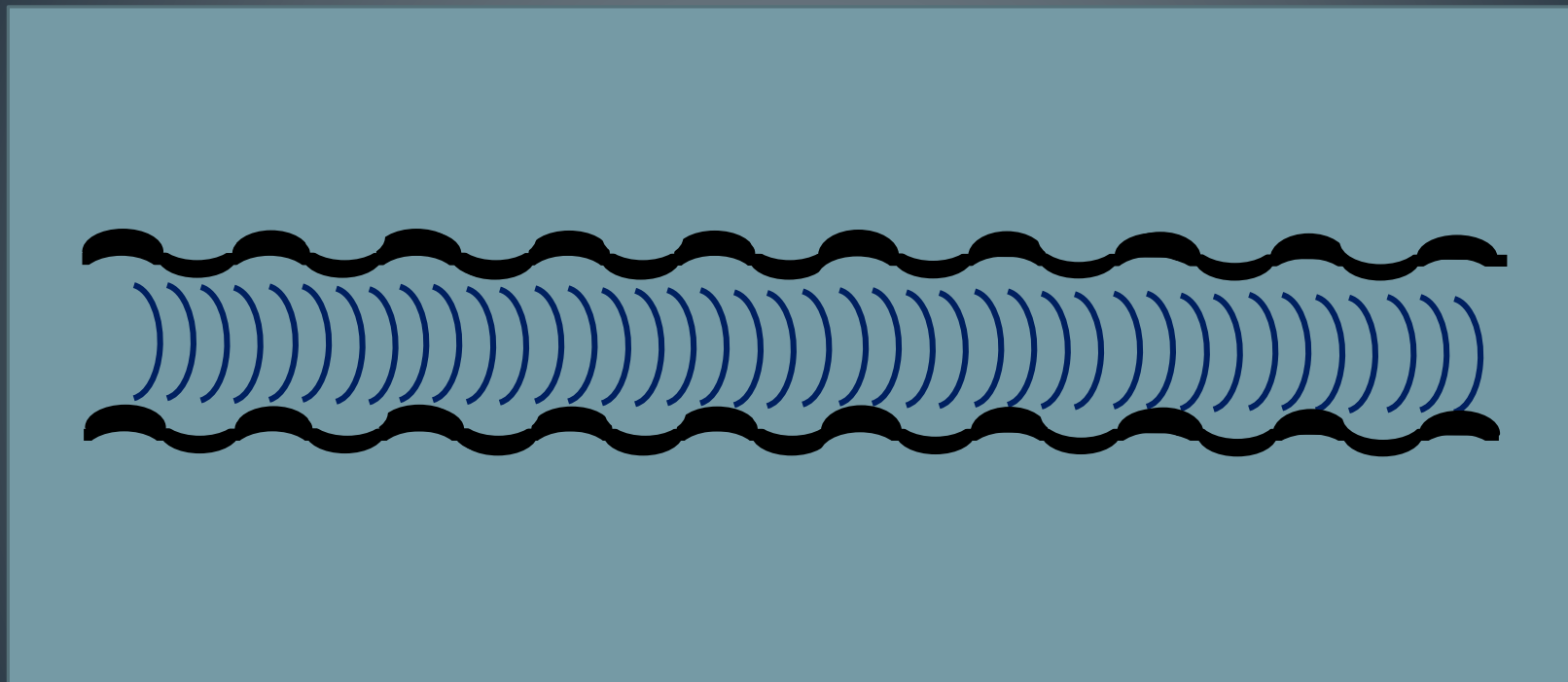


- Data was collected from a Scanning Laser Doppler Vibrometer (SLDV) while acoustic waves were excited in the panel with a contact transducer
- Goal: to correlate the SLDV data to the size and depth of the delaminations in the composite

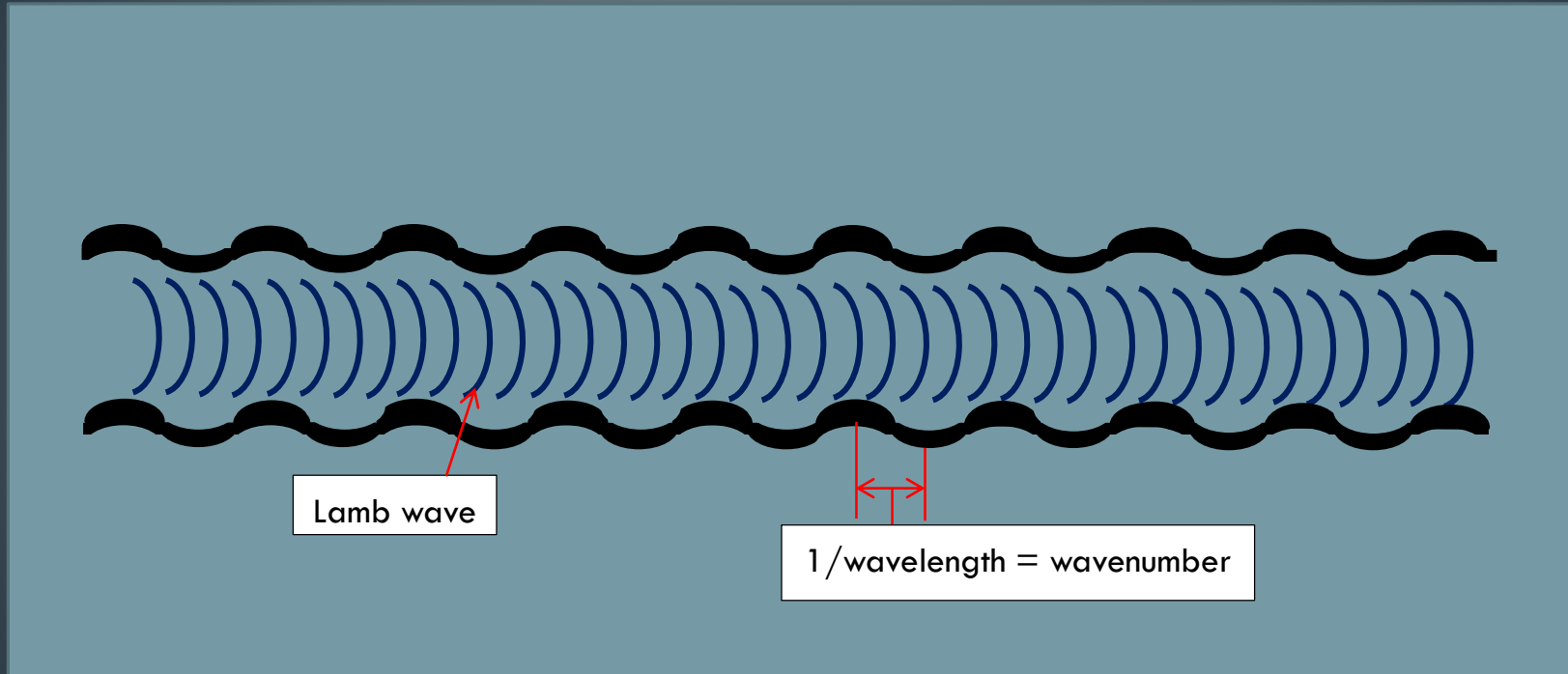


What are we detecting?

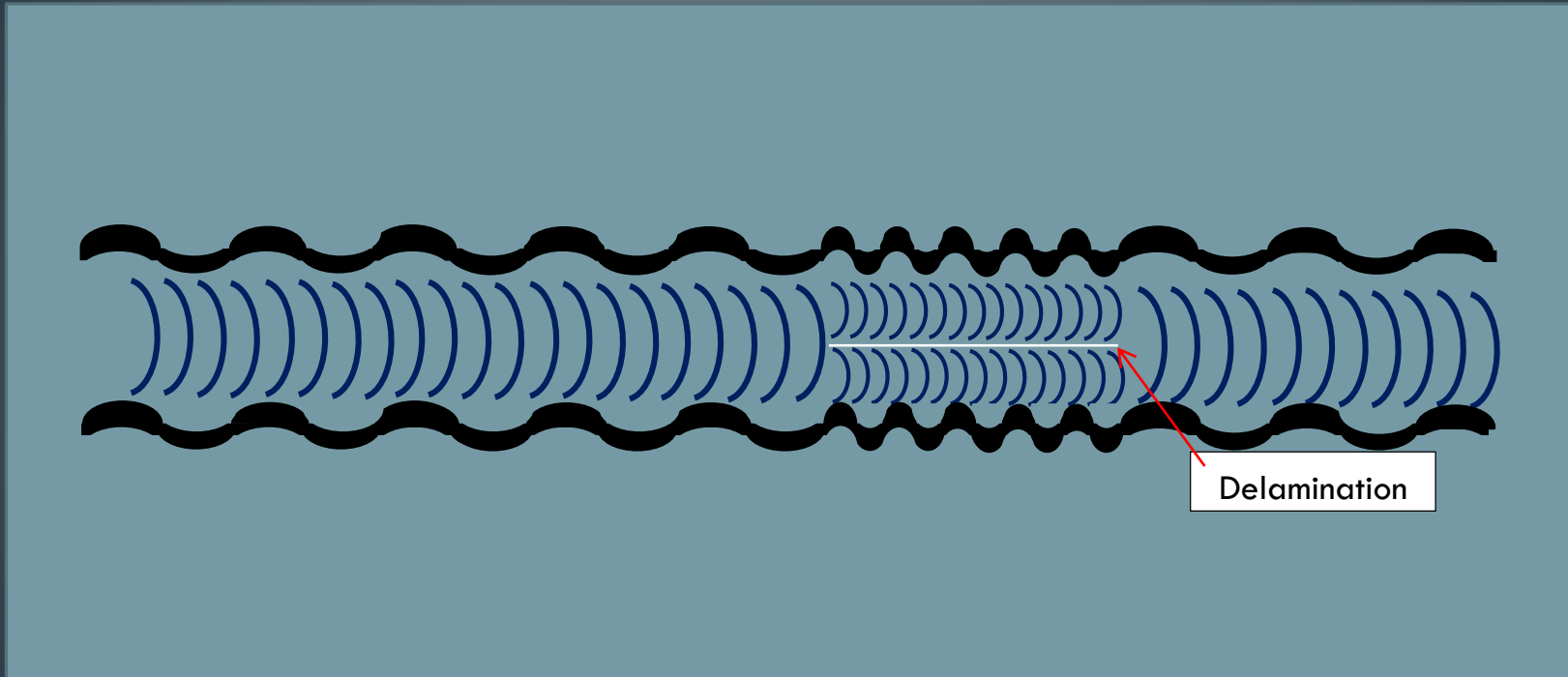
Nondestructive
Evaluation
Sciences Branch



What are we detecting?

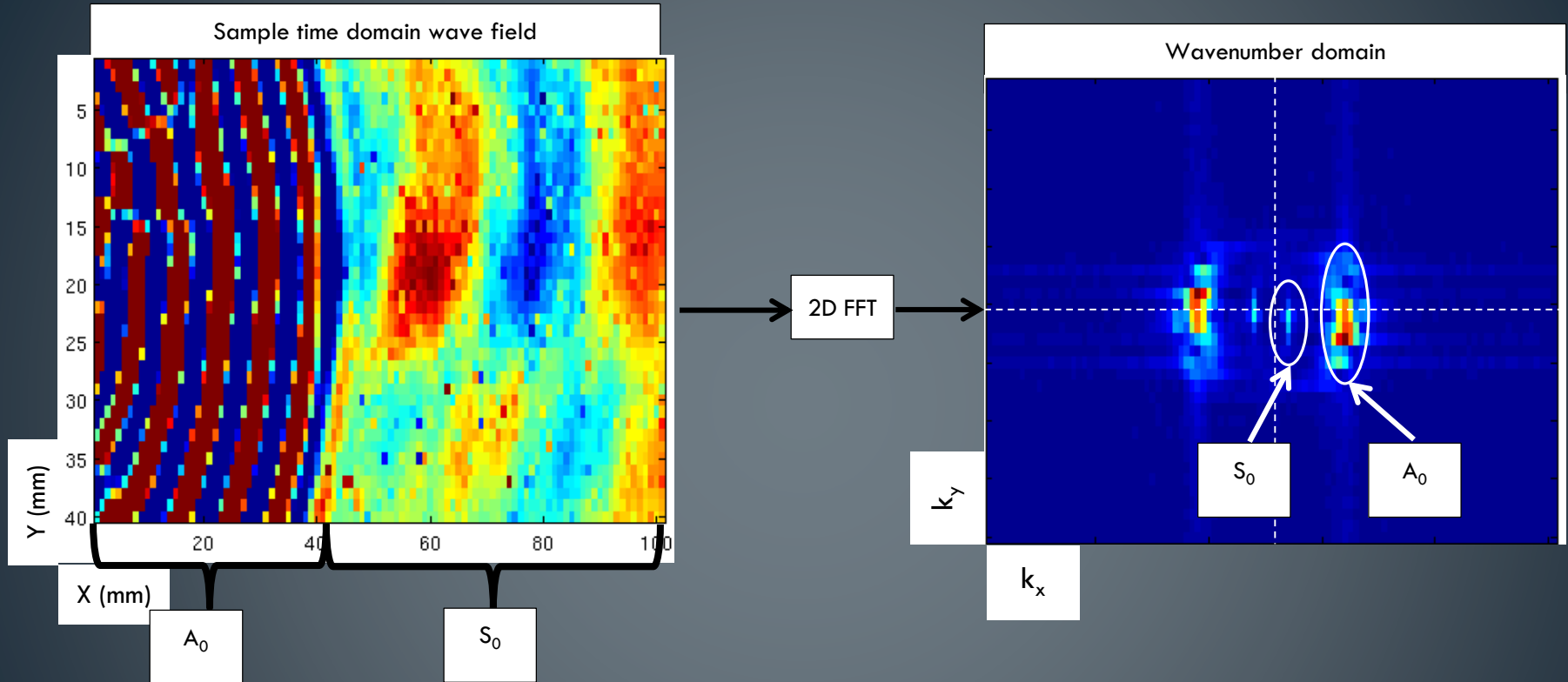


What are we detecting?



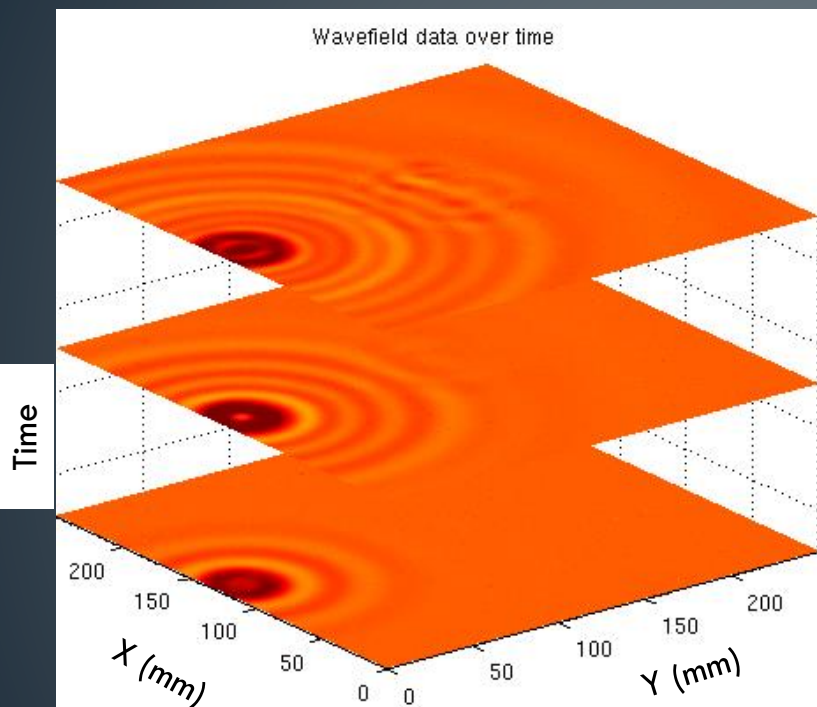
Delamination

Wavenumber Domain Analysis



Any relationship between wavenumber and location is lost

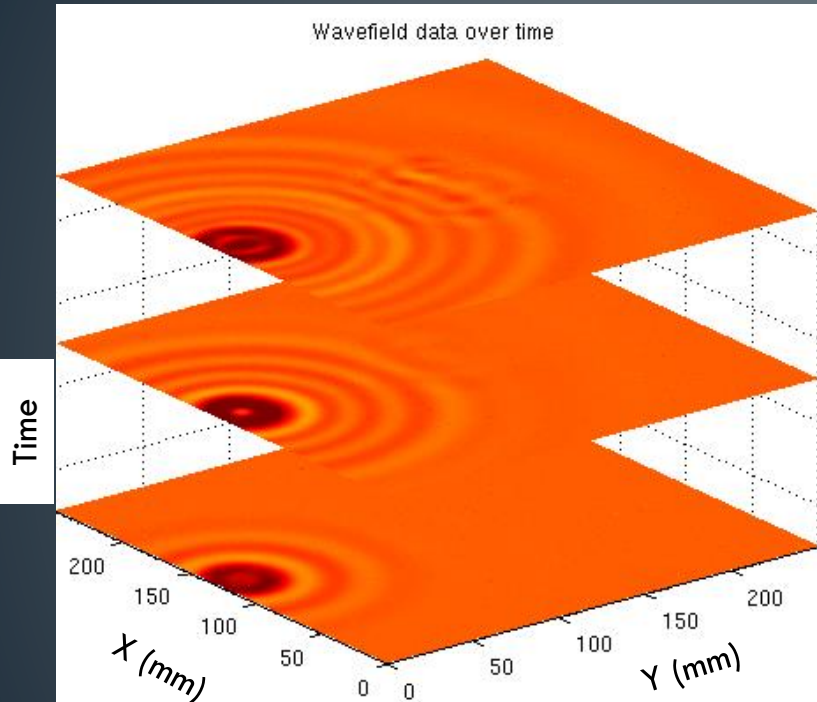
Local wavenumber technique



Local wavenumber technique

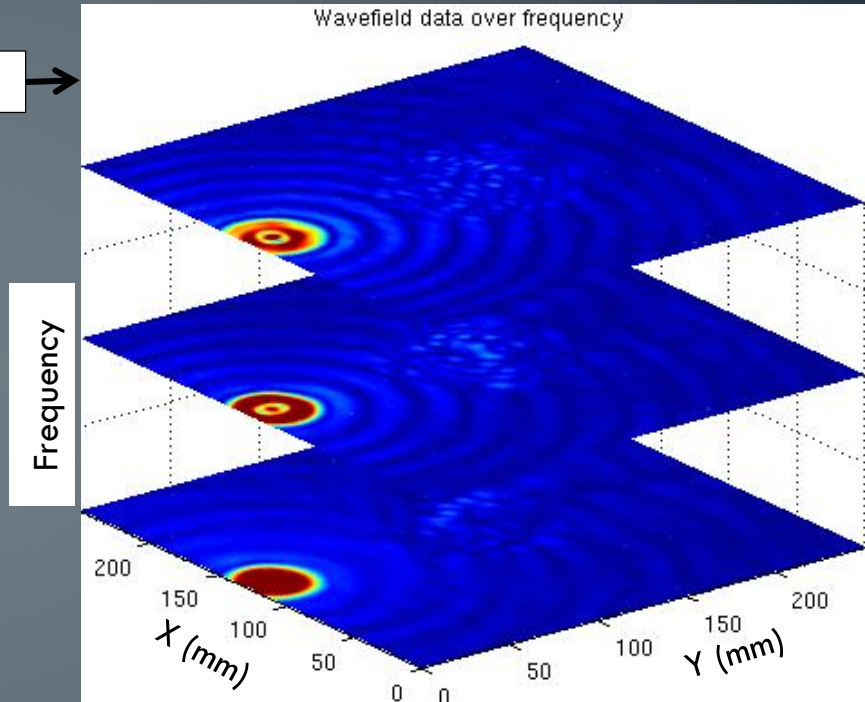


Wavefield data over time

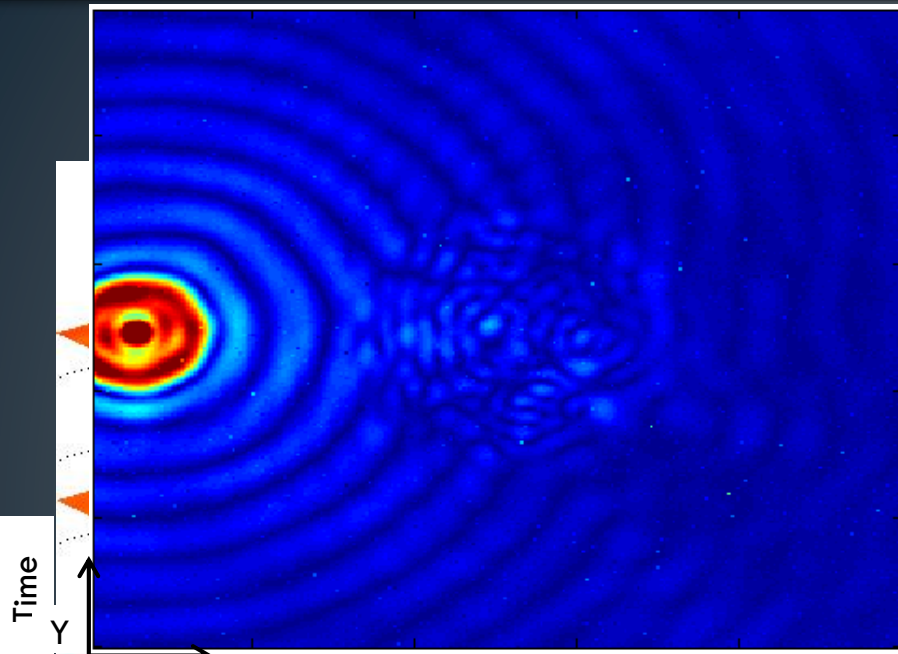


FFT

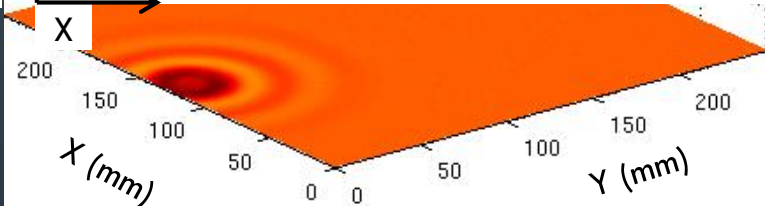
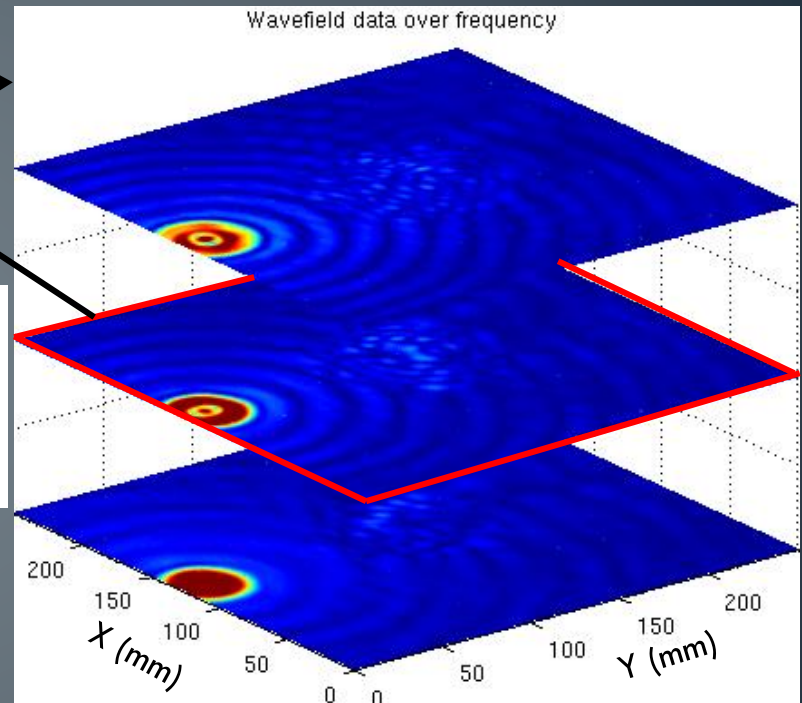
Wavefield data over frequency



Local wavenumber technique

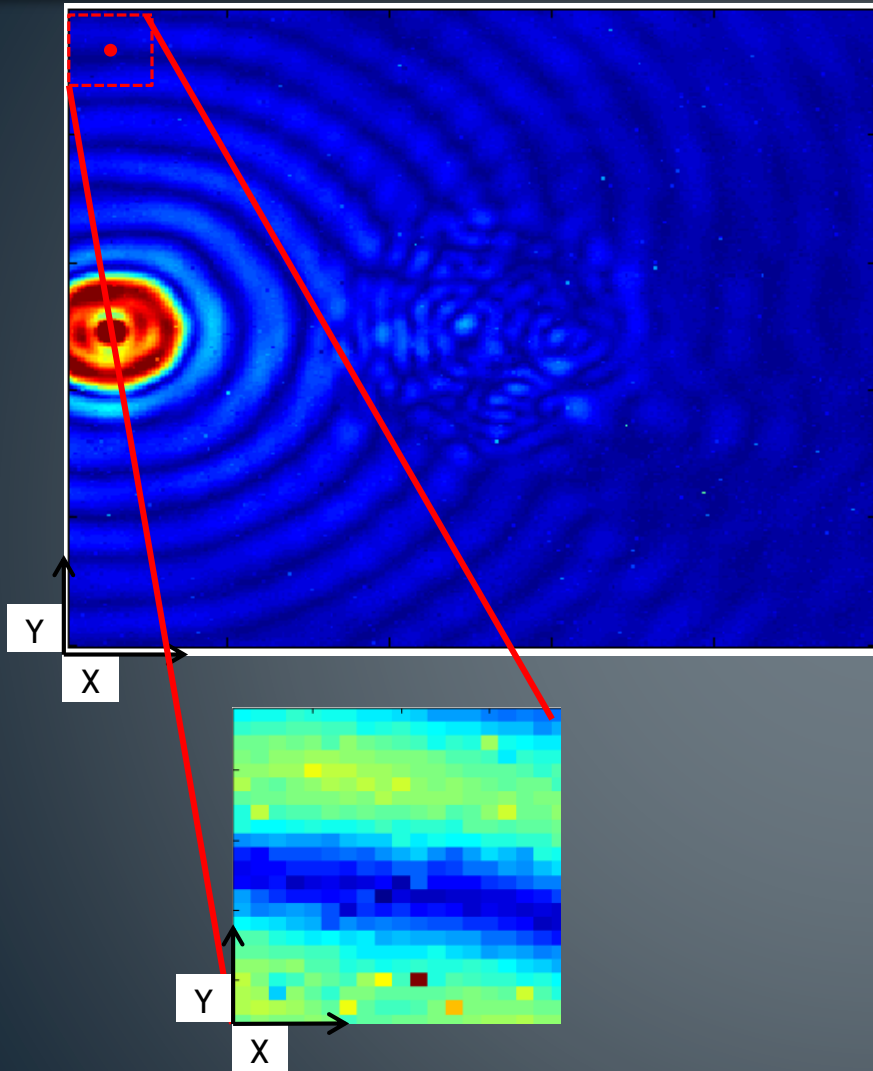


FFT

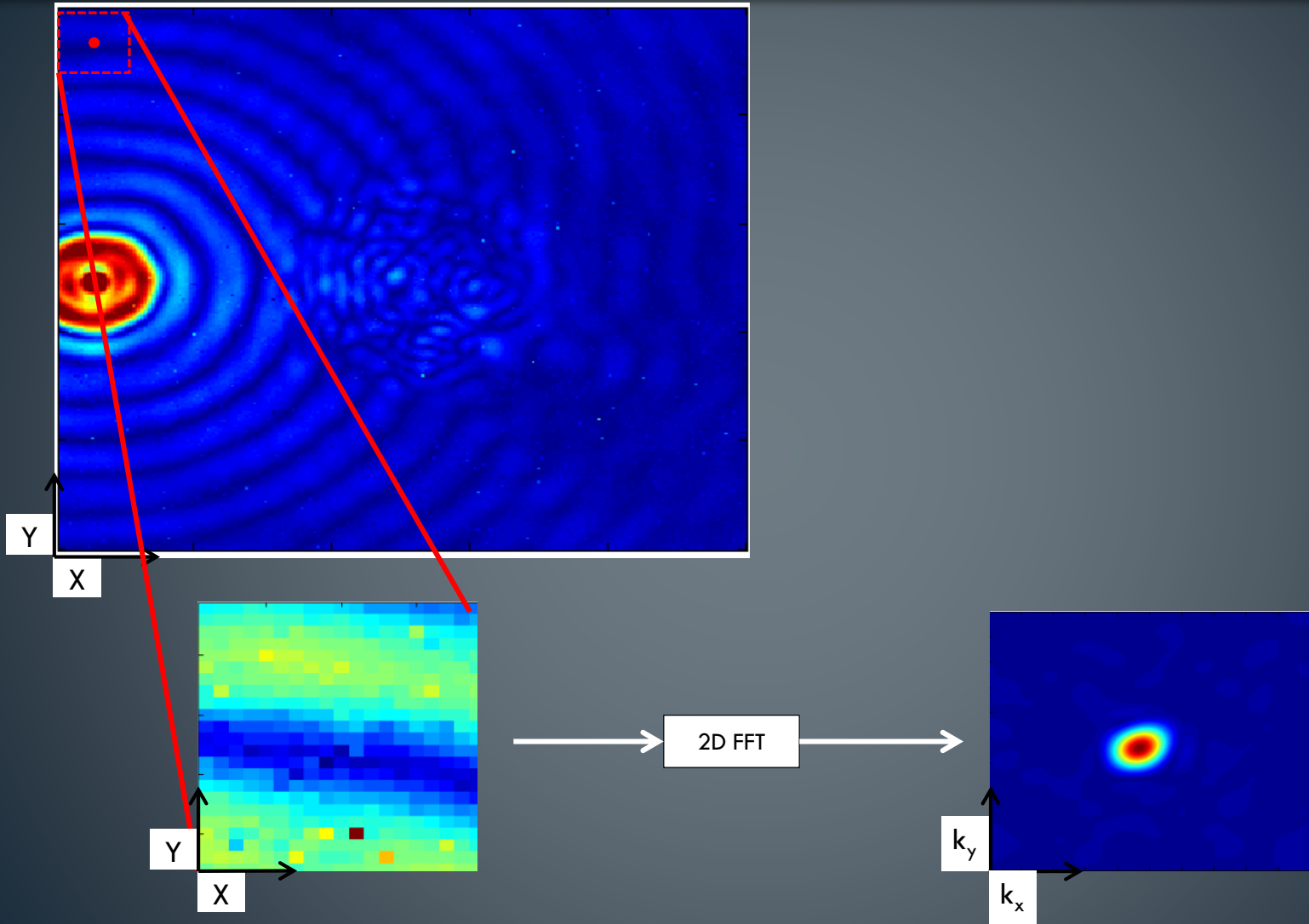


Local wavenumber technique

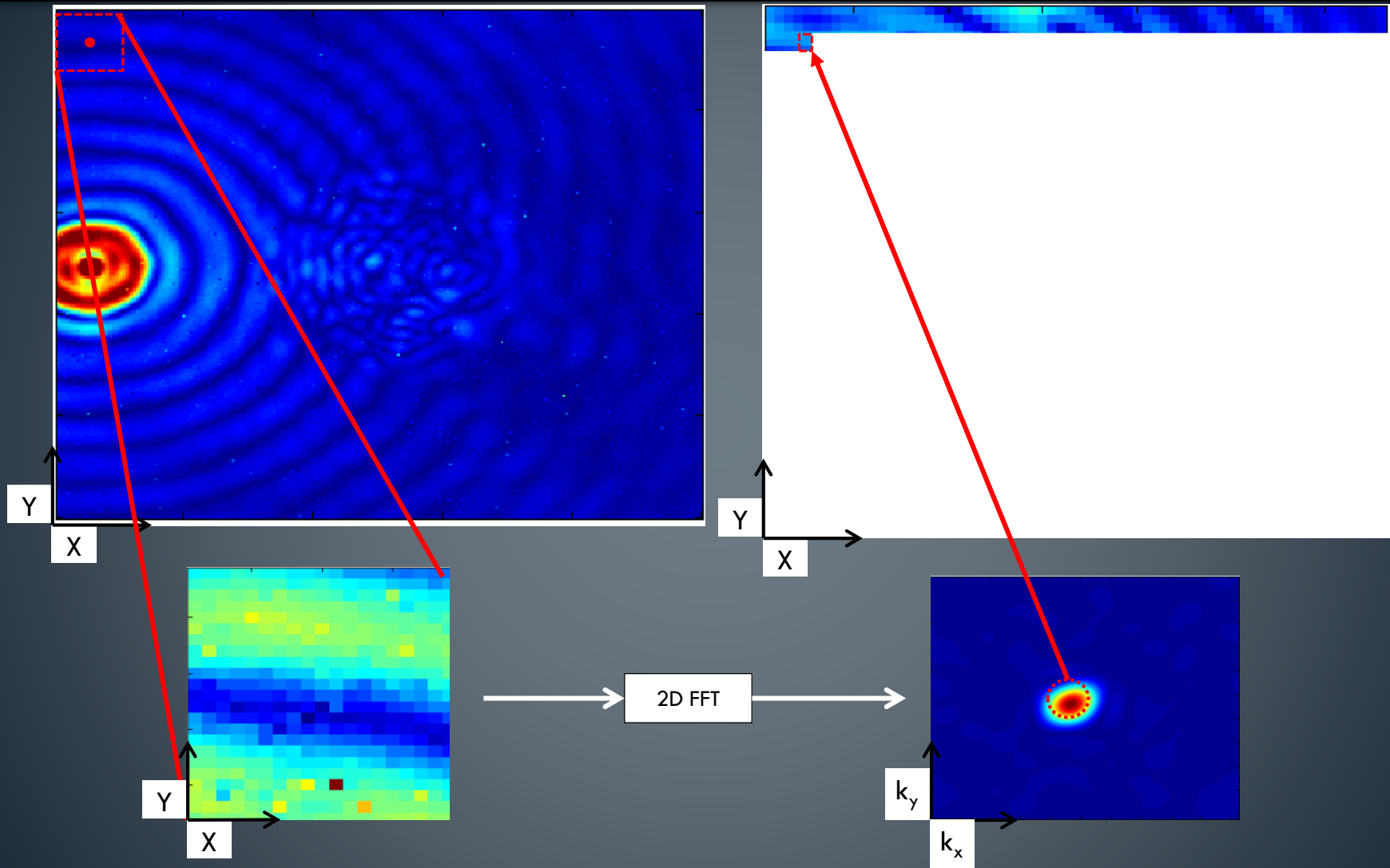
Nondestructive
Evaluation
Sciences Branch



Local wavenumber technique

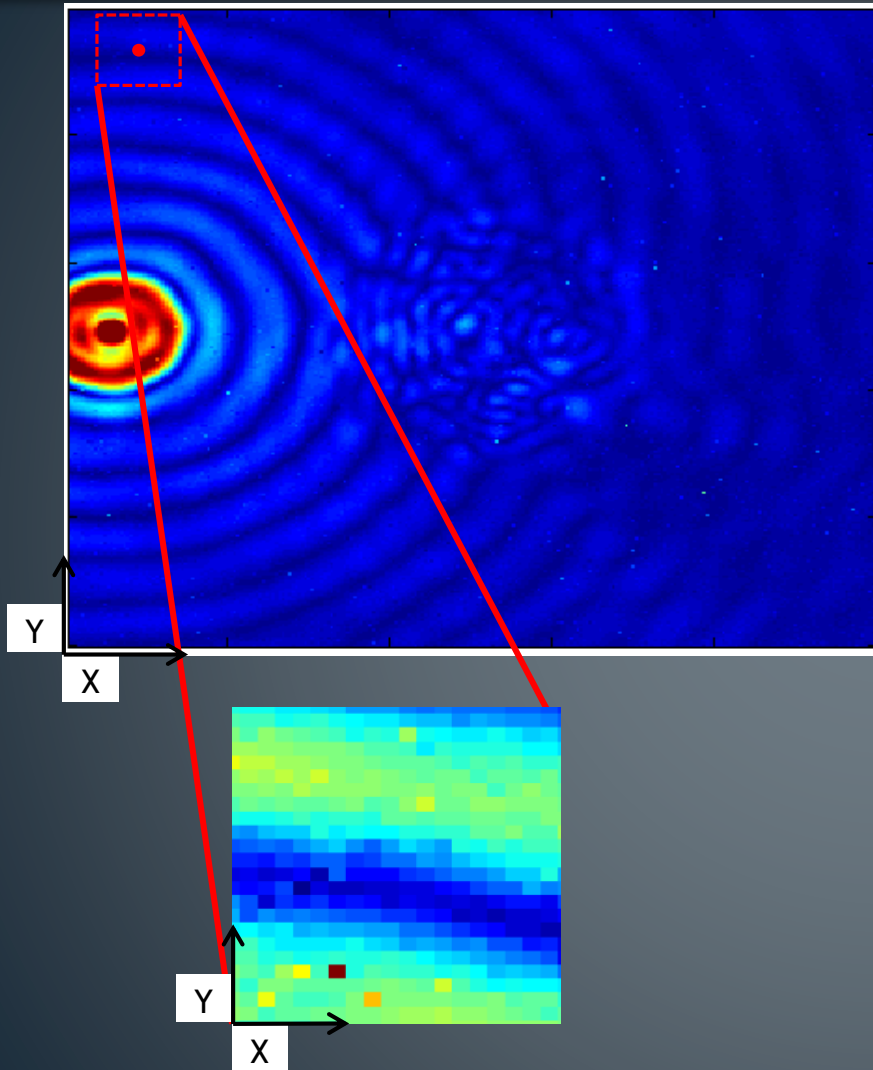


Local wavenumber technique

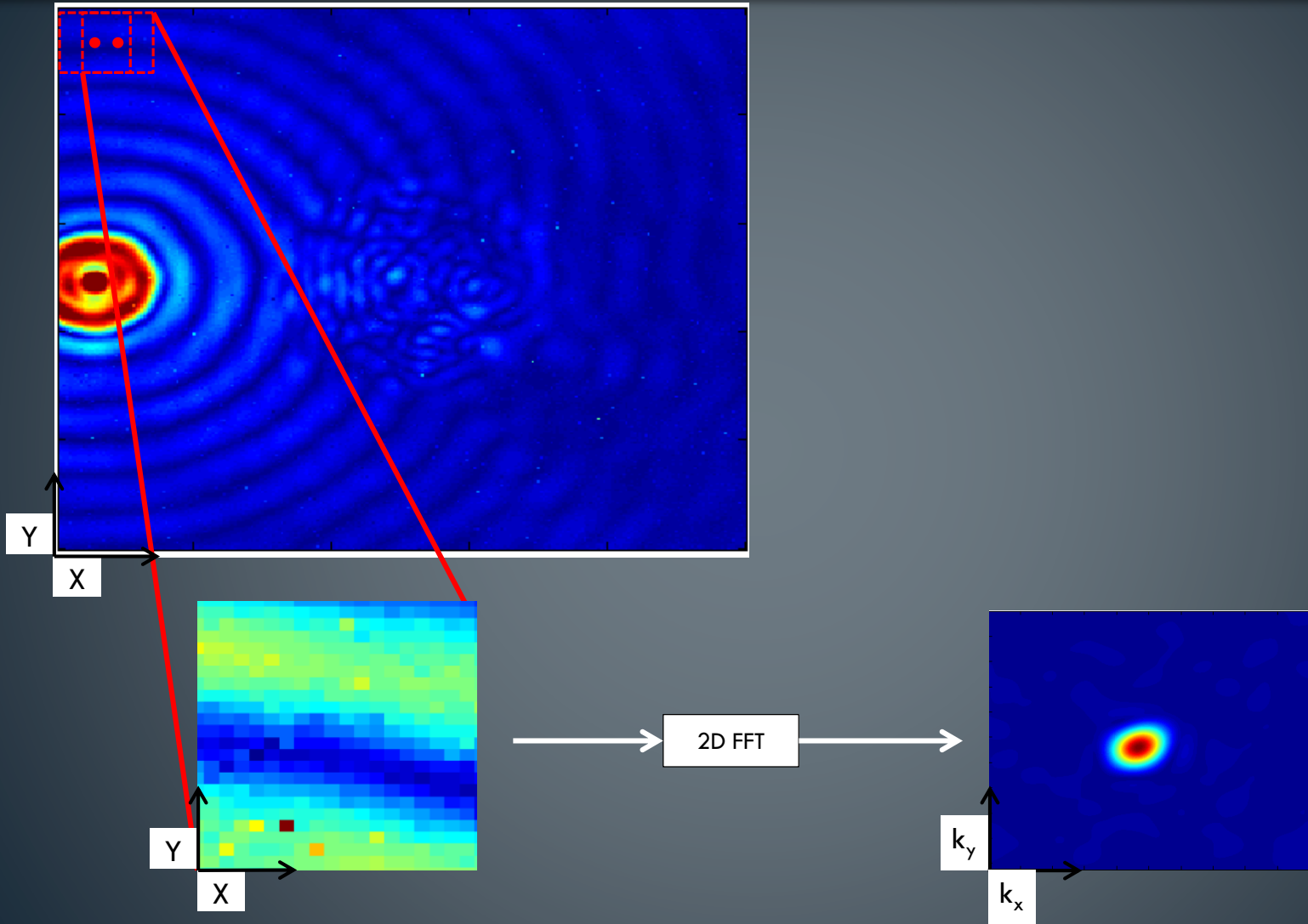


Local wavenumber technique

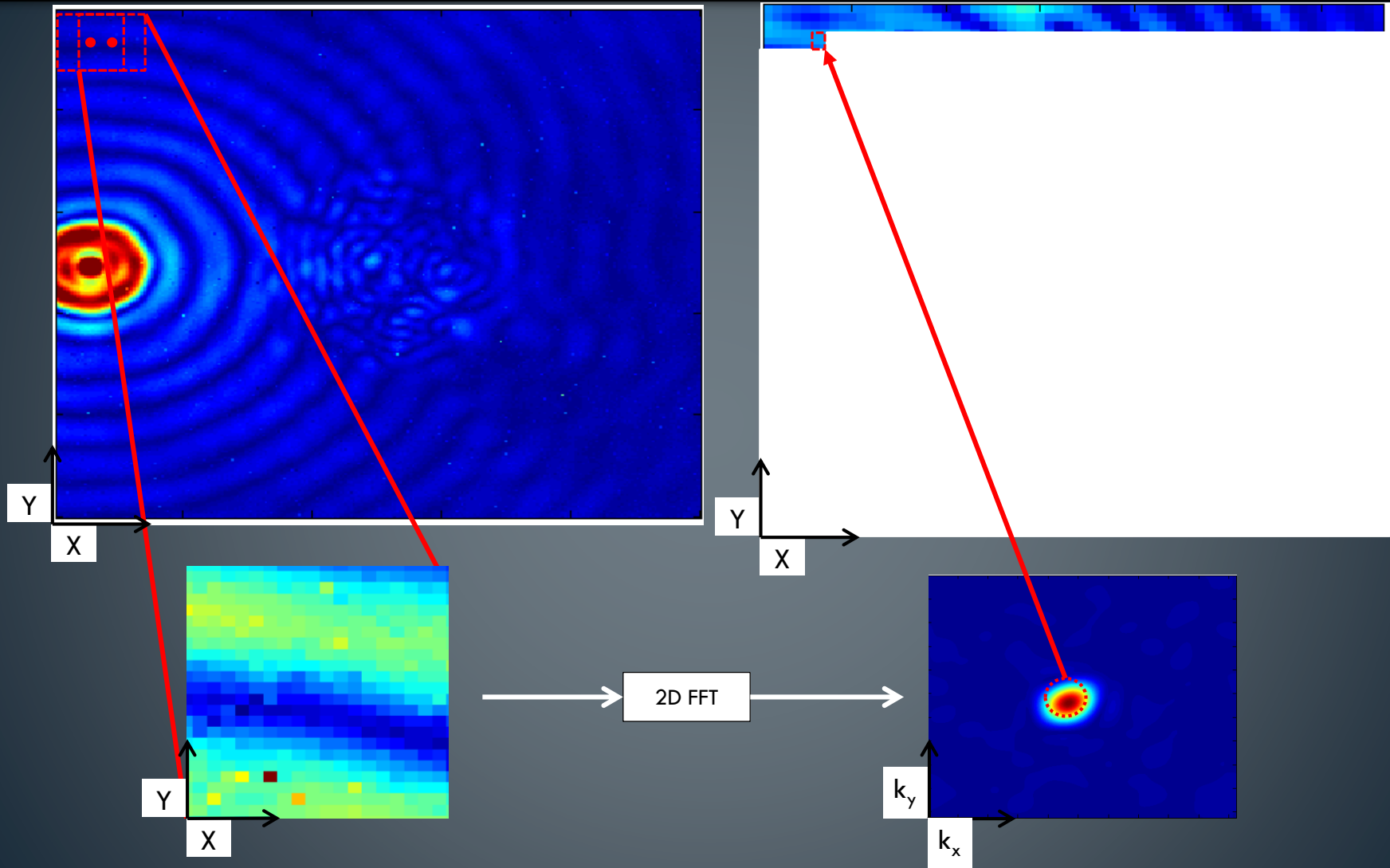
Nondestructive
Evaluation
Sciences Branch



Local wavenumber technique

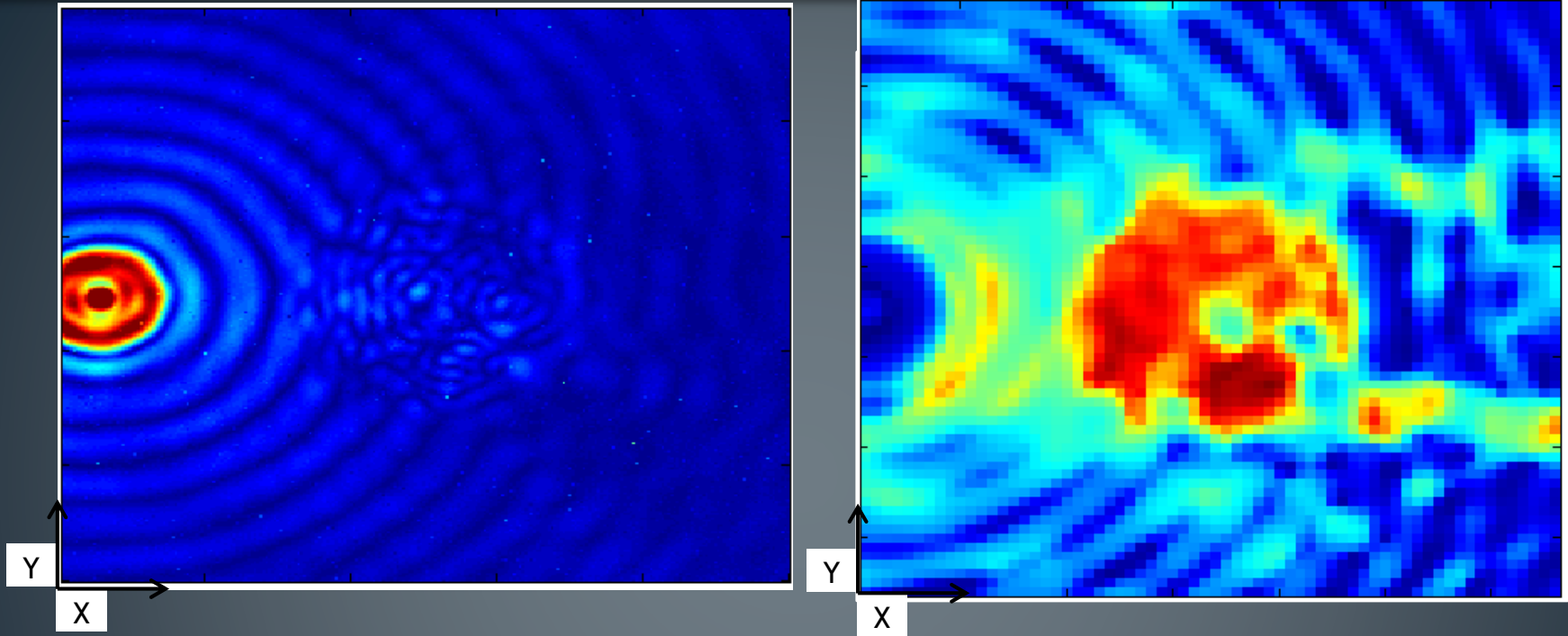


Local wavenumber technique

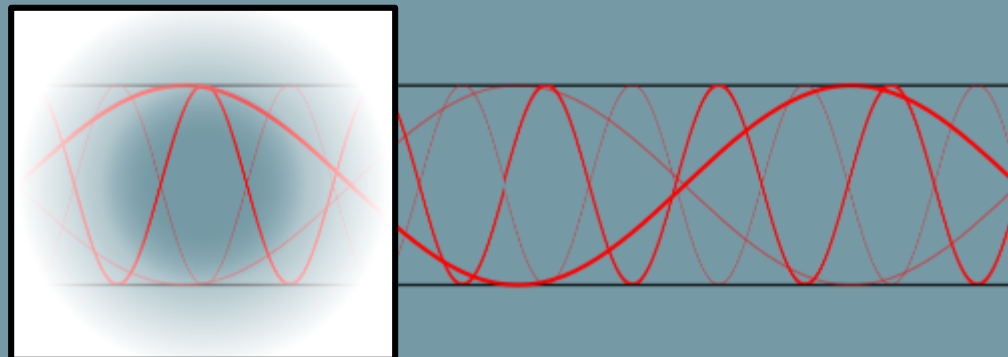
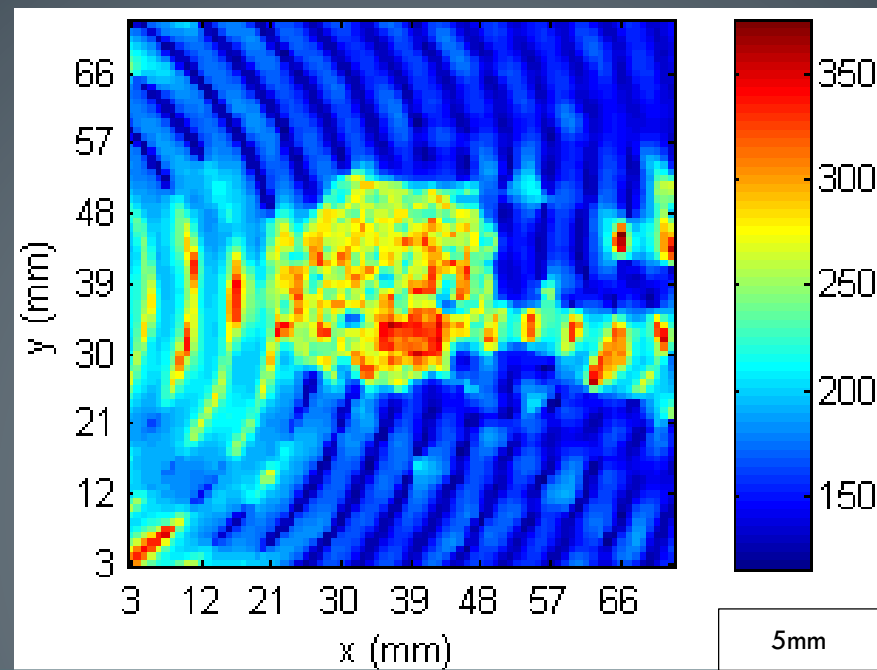


Local wavenumber technique

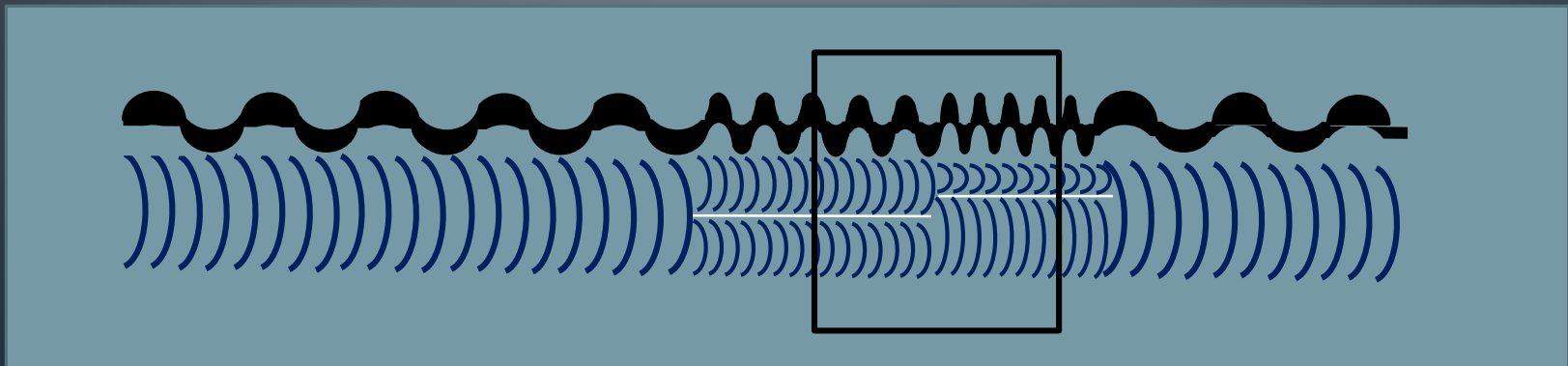
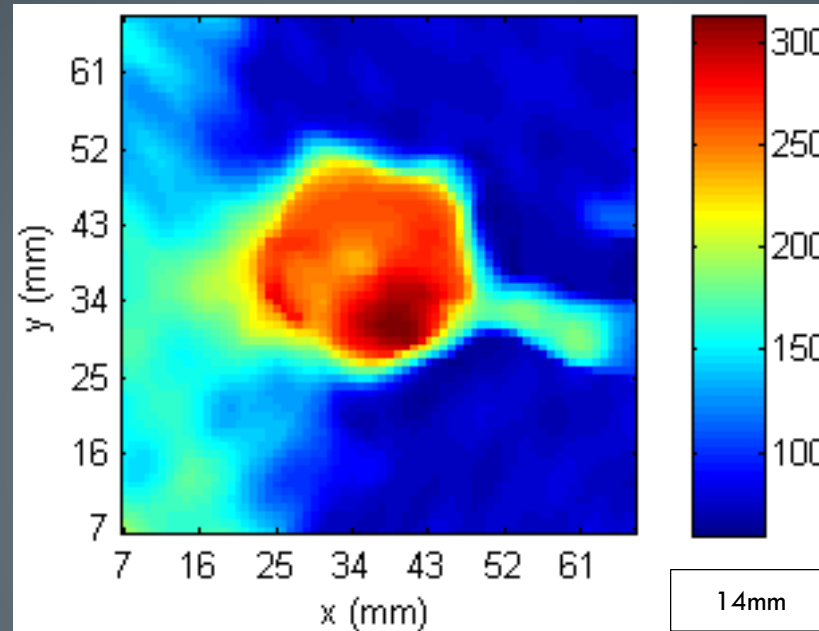
Nondestructive
Evaluation
Sciences Branch



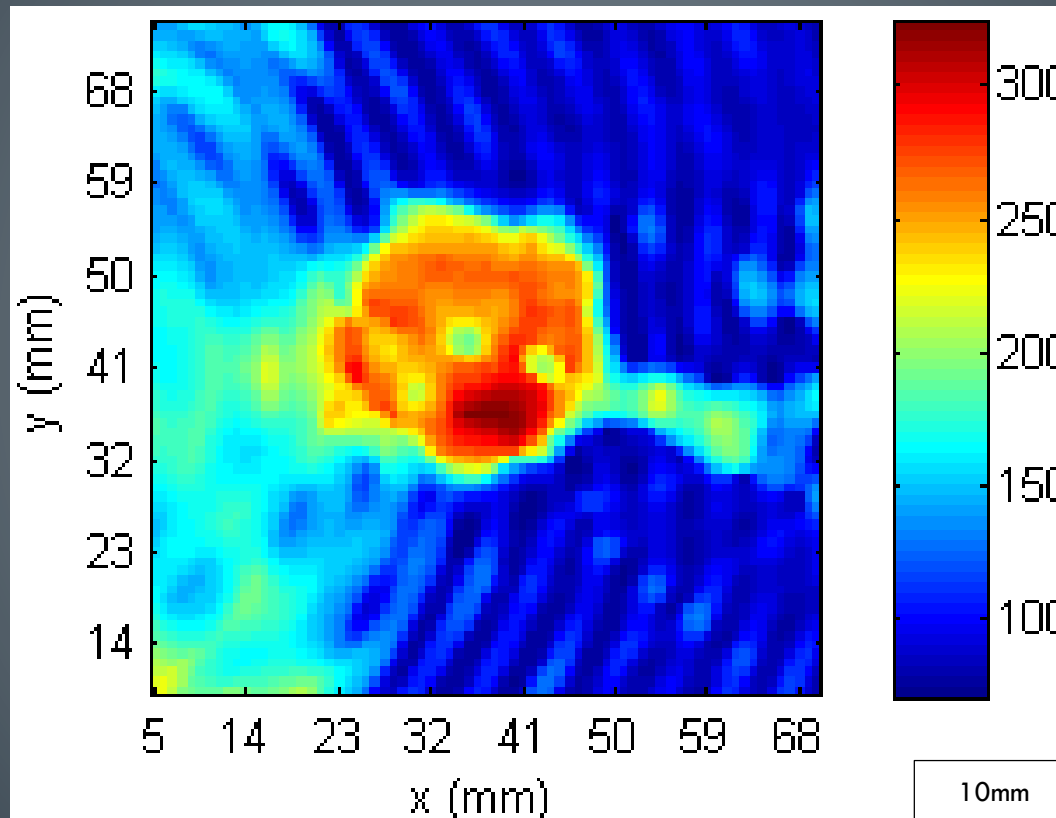
Window size



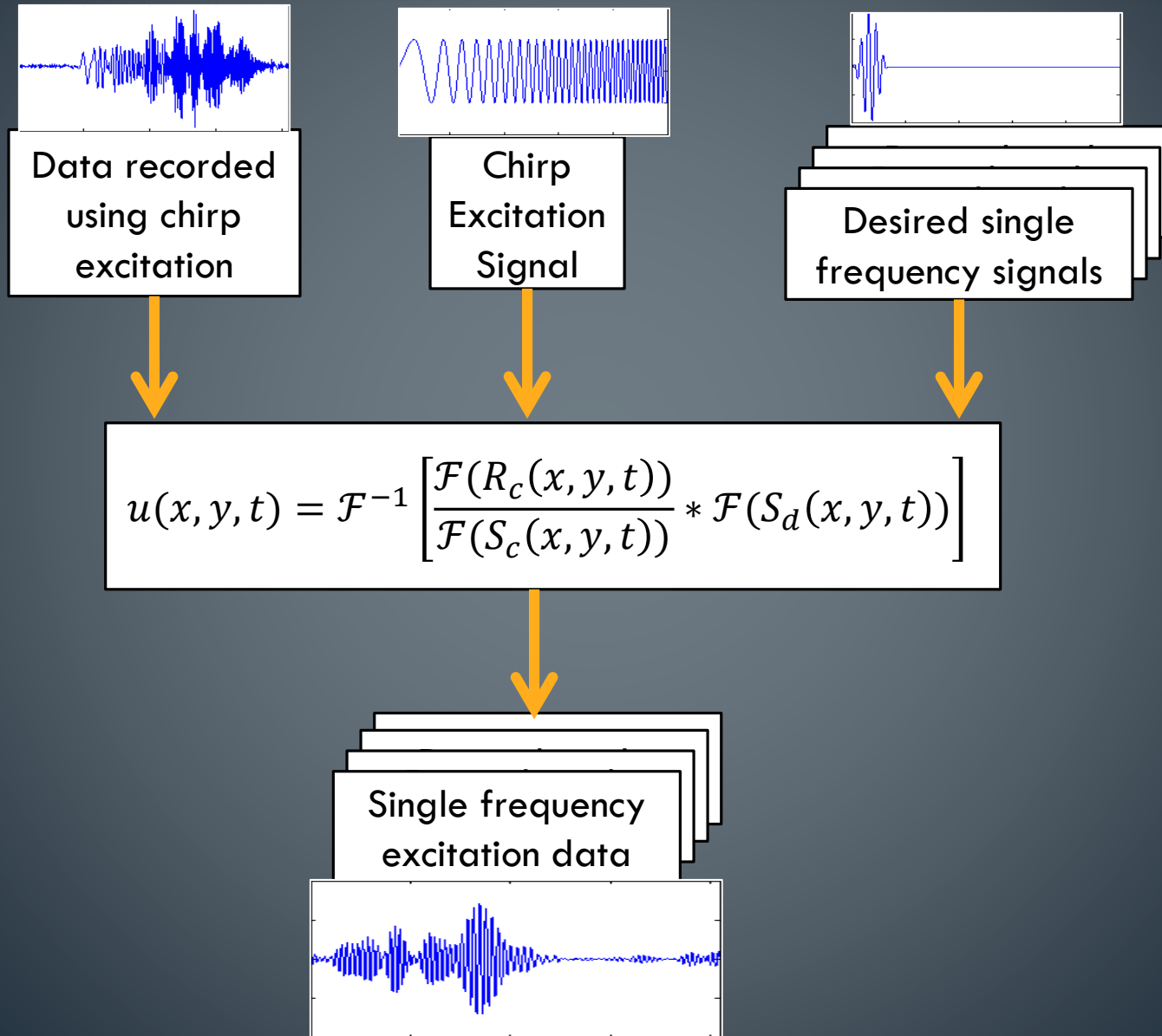
Window size



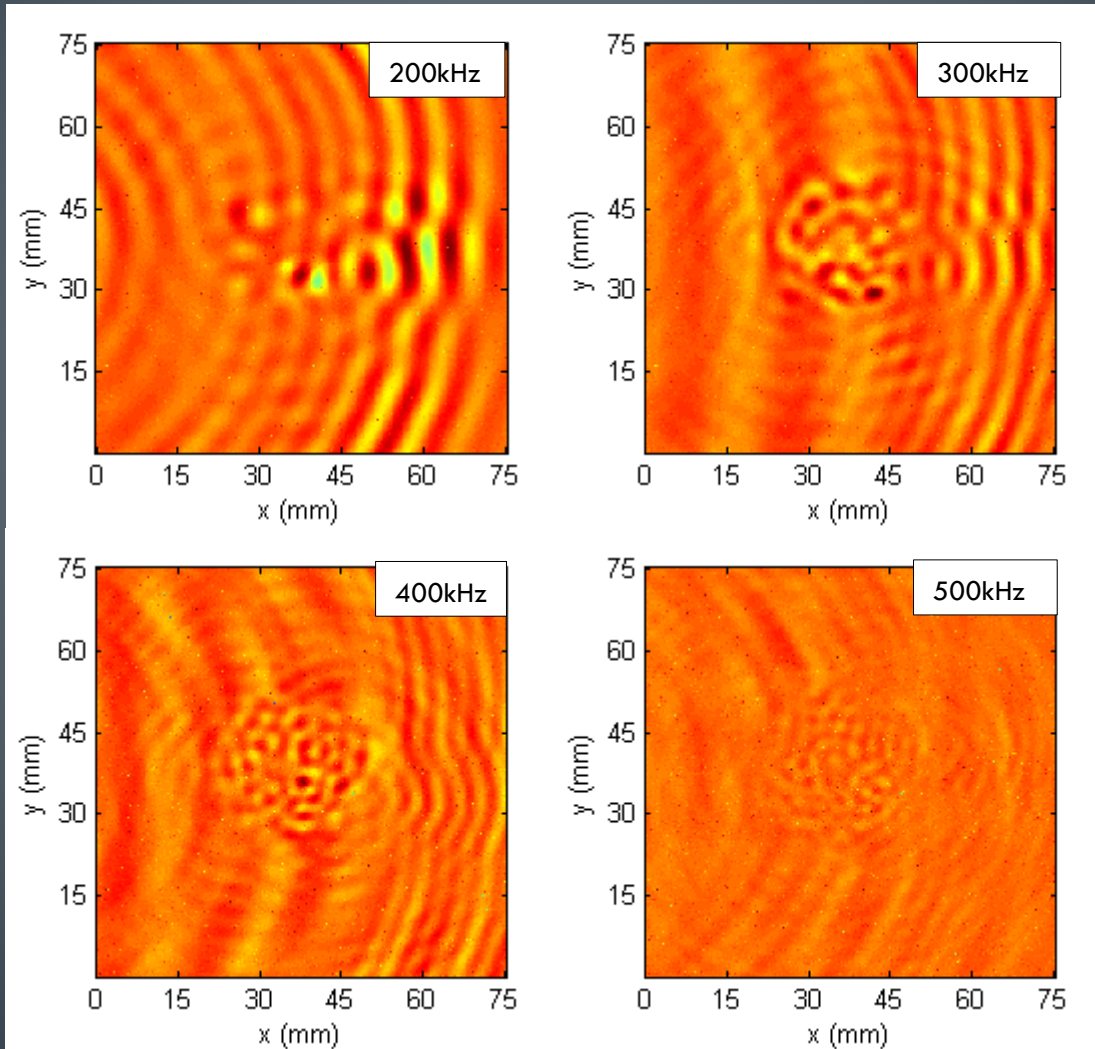
Window size



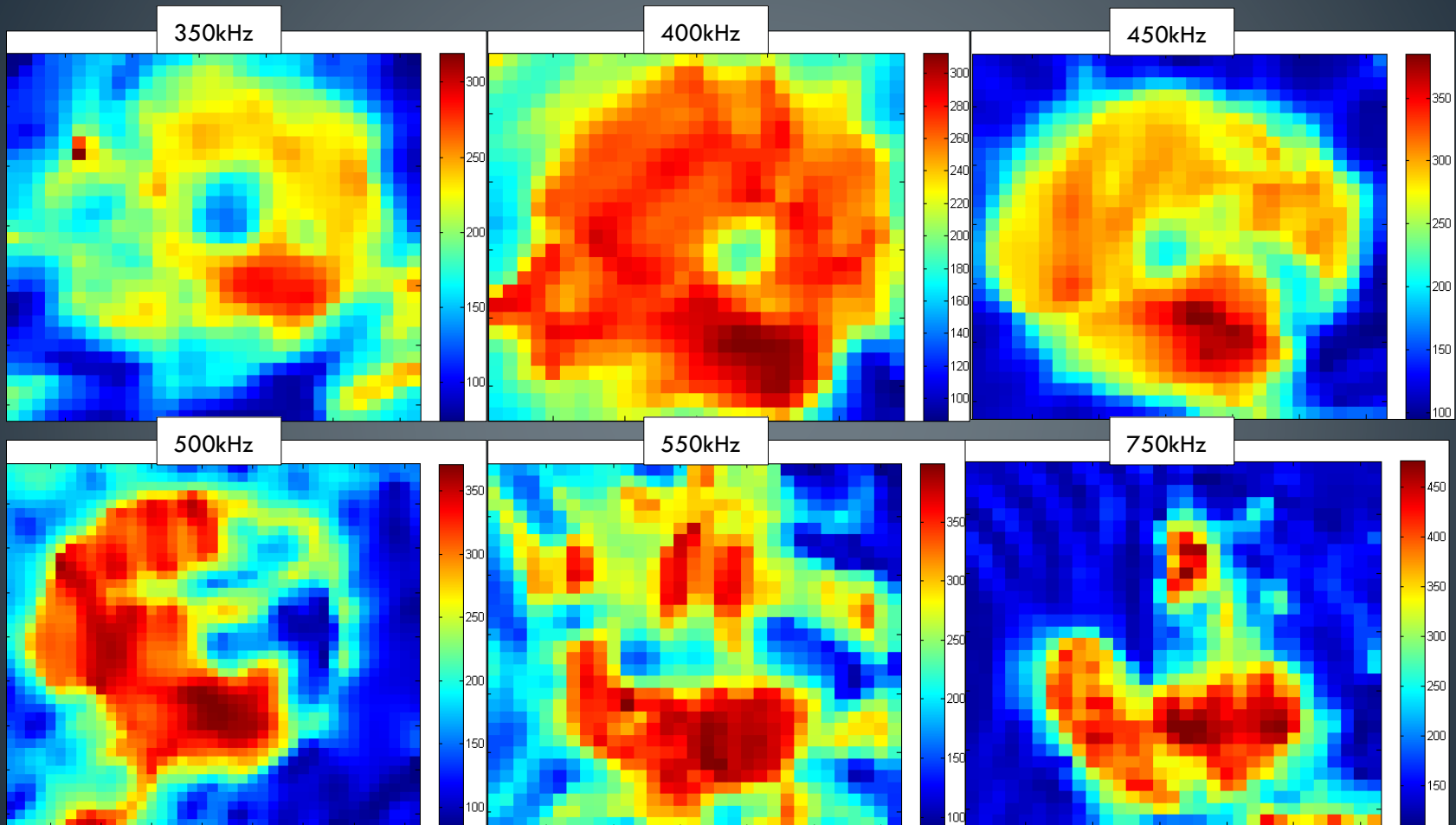
Dechirp process



Differences in frequencies: Wavefields



Differences in frequencies: Wavenumber



$$\rho \frac{\partial^2 u_1}{\partial t^2} = \frac{\partial \sigma_{11}}{\partial x_1} + \frac{\partial \sigma_{12}}{\partial x_2} + \frac{\partial \sigma_{13}}{\partial x_3}$$

$$\rho \frac{\partial^2 u_2}{\partial t^2} = \frac{\partial \sigma_{21}}{\partial x_1} + \frac{\partial \sigma_{22}}{\partial x_2} + \frac{\partial \sigma_{23}}{\partial x_3}$$

$$\rho \frac{\partial^2 u_3}{\partial t^2} = \frac{\partial \sigma_{31}}{\partial x_1} + \frac{\partial \sigma_{32}}{\partial x_2} + \frac{\partial \sigma_{33}}{\partial x_3}$$

$$\sigma_{11} = \lambda \Delta + 2\mu \epsilon_{11}$$

$$\sigma_{12} = \mu \epsilon_{12}$$

$$\epsilon_{11} = \frac{\partial u_1}{\partial x_1}$$

$$\epsilon_{12} = \frac{\partial u_1}{\partial x_2} + \frac{\partial u_2}{\partial x_1}$$

$$\rho \frac{\partial^2 u_1}{\partial t^2} = (\lambda + \mu) \frac{\partial}{\partial x_1} \left(\frac{\partial u_1}{\partial x_1} + \frac{\partial u_2}{\partial x_2} + \frac{\partial u_3}{\partial x_3} \right) + \mu \nabla^2 u_1$$

$$\rho \frac{\partial^2 u_2}{\partial t^2} = (\lambda + \mu) \frac{\partial}{\partial x_2} \left(\frac{\partial u_1}{\partial x_1} + \frac{\partial u_2}{\partial x_2} + \frac{\partial u_3}{\partial x_3} \right) + \mu \nabla^2 u_2$$

$$\rho \frac{\partial^2 u_3}{\partial t^2} = (\lambda + \mu) \frac{\partial}{\partial x_3} \left(\frac{\partial u_1}{\partial x_1} + \frac{\partial u_2}{\partial x_2} + \frac{\partial u_3}{\partial x_3} \right) + \mu \nabla^2 u_3$$

$$\sigma_{22} = \lambda \Delta + 2\mu \epsilon_{22}$$

$$\sigma_{23} = \mu \epsilon_{23}$$

$$\epsilon_{22} = \frac{\partial u_2}{\partial x_2}$$

$$\epsilon_{23} = \frac{\partial u_2}{\partial x_3} + \frac{\partial u_3}{\partial x_2}$$

$$u_1 = \pm \zeta_1 A_{L\pm} F e^{\pm i \zeta_1 x}$$

$$u_3 = \xi A_{L\pm} F e^{\pm i \zeta_1 x}$$

$$\sigma_{11} = i \rho (\omega^2 - 2c_2^2 \xi^2) A_{L\pm} F e^{\pm i \zeta_1 x}$$

$$\sigma_{22} = i \rho \omega^2 (1 - 2c_2^2/c_1^2) A_{L\pm} F e^{\pm i \zeta_1 x}$$

$$\sigma_{33} = i \rho (\omega^2 - 2c_2^2 \zeta_1^2) A_{L\pm} F e^{\pm i \zeta_1 x}$$

$$u_1(b) = \frac{-\sigma_{11}}{k_{11}} = -\nabla \phi = \begin{bmatrix} \frac{\partial \phi}{\partial x_1} \\ \frac{\partial \phi}{\partial x_2} \\ \frac{\partial \phi}{\partial x_3} \end{bmatrix}$$

$$u_2(b) = \frac{-\sigma_{12}}{k_{12}}$$

$$u_3(b) = \frac{-\sigma_{13}}{k_{13}}$$

$$u_L = \nabla \phi = \begin{bmatrix} k_1 \\ 0 \\ k_3 \end{bmatrix} A_L e^{i(\mathbf{k} \cdot \mathbf{x} - \omega t)}$$

$$u_S = \nabla \times \mathbf{H} = \begin{bmatrix} \frac{\partial}{\partial x_1} \\ \frac{\partial}{\partial x_2} \\ \frac{\partial}{\partial x_3} \end{bmatrix} \times \begin{bmatrix} 0 \\ H_3 \\ 0 \end{bmatrix}$$

$$\begin{bmatrix} u_1 \\ u_3 \\ \sigma_{11} \\ \sigma_{13} \end{bmatrix} = \begin{bmatrix} \zeta_1 g \zeta_1 \\ \xi g \zeta_1 \\ i \rho (\omega^2 - 2c_2^2 \xi^2) g \zeta_1 \\ 2i \rho \xi c_2^2 \zeta_1 g \zeta_1 \end{bmatrix} \frac{i \rho \omega}{-2}$$

$$\begin{bmatrix} C_{11} \xi^2 + C_{66} k_x^2 + 2C_{16} \xi k_x - \rho \omega^2 & C_{16} \xi^2 \\ \Gamma_{12} & C_{66} \xi^2 \\ \Gamma_{13} & \end{bmatrix}$$

$$e^{i(\zeta x_3 - \omega t)} + A_{S2} \begin{bmatrix} -i \zeta \cos(\zeta_2 x_2) \\ 0 \\ \zeta_2 \cos(\zeta_2 x_2) \end{bmatrix} e^{i(\zeta x_3 - \omega t)}$$

$$(\zeta_2^2 - \xi^2)^2 \cos(\zeta_1 d/2) \sin(\zeta_2 d/2)$$

$$[S] (\zeta_2^2 - \xi^2)^2 \sin(\zeta_1 d/2) \cos(\zeta_2 d/2) + 4\xi^2 \zeta_1 \zeta_2 \cos(\zeta_1 d/2) \sin(\zeta_2 d/2) - 2i \rho \xi c_2^2 \zeta_2 g \zeta_2 + i \frac{\rho L \zeta_1 \omega^4}{\rho S \gamma c_2^4} \cos(\zeta_1 d/2) \cos(\zeta_2 d/2)$$

$$\mathbf{T} = \begin{pmatrix} \sigma_{yy} \\ \sigma_{zz} \\ \sigma_{yz} \\ \sigma_{zx} \\ \sigma_{xy} \end{pmatrix} = \begin{bmatrix} C_{11} & C_{12} & C_{13} & 0 & 0 \\ C_{21} & C_{22} & C_{23} & 0 & 0 \\ C_{31} & C_{32} & C_{33} & 0 & 0 \\ 0 & 0 & 0 & C_{44} & 0 \\ 0 & 0 & 0 & 0 & C_{55} \end{bmatrix}$$

$$(7.58)$$

$$e^{i(\zeta x_3 - \omega t)} + A_{L2} \begin{bmatrix} \zeta_1 \cos(\zeta_1 x_2) \\ 0 \\ i \xi \sin(\zeta_1 x_2) \end{bmatrix} \mathbf{S} = \begin{bmatrix} 0 \\ H_3 \\ 0 \end{bmatrix} \begin{bmatrix} C_{11} \xi^2 + C_{66} k_x^2 + 2C_{16} \xi k_x - \rho \omega^2 \\ \Gamma_{12} \\ \Gamma_{13} \end{bmatrix}$$

$$e^{i(\zeta x_3 - \omega t)} + A_{S2} \begin{bmatrix} -i \xi \sin(\zeta_2 x_2) \\ 0 \\ \zeta_2 \cos(\zeta_2 x_2) \end{bmatrix} e^{i(\zeta x_3 - \omega t)}$$

$$(\zeta_2^2 - \xi^2)^2 \cos(\zeta_1 d/2) \sin(\zeta_2 d/2)$$

$$[S] (\zeta_2^2 - \xi^2)^2 \sin(\zeta_1 d/2) \cos(\zeta_2 d/2) + 4\xi^2 \zeta_1 \zeta_2 \cos(\zeta_1 d/2) \sin(\zeta_2 d/2) - 2i \rho \xi c_2^2 \zeta_2 g \zeta_2 + i \frac{\rho L \zeta_1 \omega^4}{\rho S \gamma c_2^4} \cos(\zeta_1 d/2) \cos(\zeta_2 d/2)$$

$$= A_{S1} \begin{bmatrix} -i \zeta \cos(\zeta_2 x_2) \\ 0 \\ -\zeta_2 \sin(\zeta_2 x_2) \end{bmatrix} e^{i(\zeta x_3 - \omega t)}$$

$$\begin{bmatrix} \zeta_1 \cos(\zeta_1 d/2) & i \xi \cos(\zeta_2 d/2) \\ \mu (\zeta_2^2 - \xi^2) \cos(\zeta_1 d/2) & 2i \mu \xi \zeta_2 \cos(\zeta_2 d/2) \\ 2i \mu \xi \zeta_1 \cos(\zeta_1 d/2) & \mu (\zeta_2^2 - \xi^2) \sin(\zeta_2 d/2) \end{bmatrix}$$

$$\begin{bmatrix} \zeta_1 \cos(\zeta_1 d/2) & i \xi \cos(\zeta_2 d/2) \\ \mu (\zeta_2^2 - \xi^2) \sin(\zeta_1 d/2) & 2i \mu \xi \zeta_2 \sin(\zeta_2 d/2) \\ 2i \mu \xi \zeta_1 \cos(\zeta_1 d/2) & \mu (\zeta_2^2 - \xi^2) \cos(\zeta_2 d/2) \end{bmatrix}$$

$$e^{i(\zeta x_3 - \omega t)} + A_{S2} \begin{bmatrix} -i \zeta \cos(\zeta_2 x_2) \\ 0 \\ \zeta_2 \cos(\zeta_2 x_2) \end{bmatrix} e^{i(\zeta x_3 - \omega t)}$$

$$(\zeta_2^2 - \xi^2)^2 \cos(\zeta_1 d/2) \sin(\zeta_2 d/2)$$

$$[S] (\zeta_2^2 - \xi^2)^2 \sin(\zeta_1 d/2) \cos(\zeta_2 d/2) + 4\xi^2 \zeta_1 \zeta_2 \cos(\zeta_1 d/2) \sin(\zeta_2 d/2) - 2i \rho \xi c_2^2 \zeta_2 g \zeta_2 + i \frac{\rho L \zeta_1 \omega^4}{\rho S \gamma c_2^4} \cos(\zeta_1 d/2) \cos(\zeta_2 d/2)$$

$$= A_{S1} \begin{bmatrix} -i \zeta \cos(\zeta_2 x_2) \\ 0 \\ -\zeta_2 \sin(\zeta_2 x_2) \end{bmatrix} e^{i(\zeta x_3 - \omega t)}$$

$$\begin{bmatrix} C_{11} & C_{12} & C_{13} & 0 & 0 \\ C_{21} & C_{22} & C_{23} & 0 & 0 \\ C_{31} & C_{32} & C_{33} & 0 & 0 \\ 0 & 0 & 0 & C_{44} & 0 \\ 0 & 0 & 0 & 0 & C_{55} \end{bmatrix}$$

$$\begin{bmatrix} -i \zeta \sin(\zeta_2 d/2) & -i \xi \cos(\zeta_2 d/2) \\ \zeta_2 \sin(\zeta_2 d/2) & -2i \mu \xi \zeta_2 \cos(\zeta_2 d/2) \\ -A_{33} & -A_{34} \\ -(\zeta_2^2 - \xi^2) \cos(\zeta_2 d/2) & -\mu (\zeta_2^2 - \xi^2) \sin(\zeta_2 d/2) \\ A_{51} & -A_{54} \end{bmatrix}$$

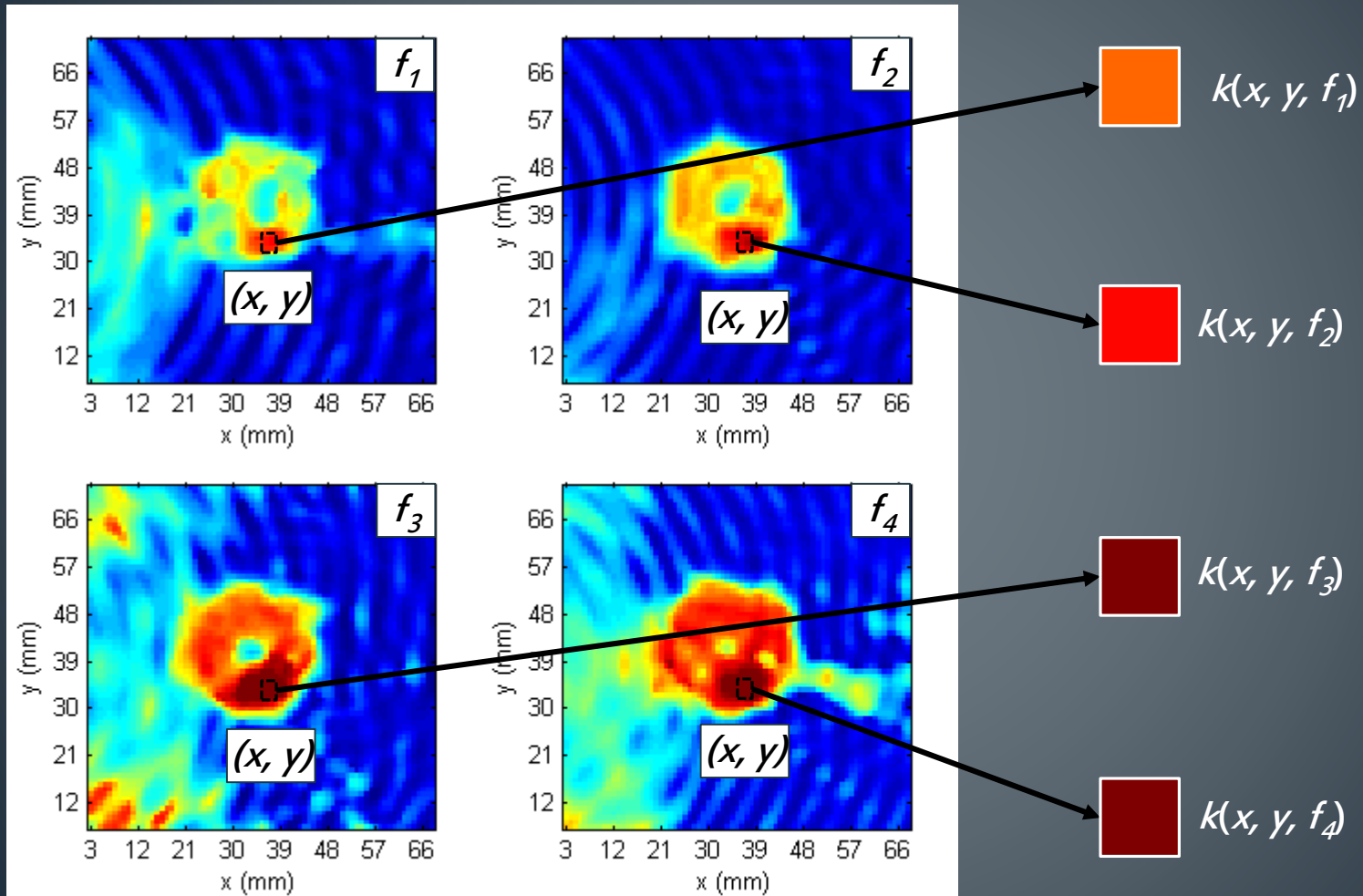
$$= A_{S1} \begin{bmatrix} -i \zeta \cos(\zeta_2 x_2) \\ 0 \\ -\zeta_2 \sin(\zeta_2 x_2) \end{bmatrix} e^{i(\zeta x_3 - \omega t)}$$

$$\begin{bmatrix} C_{11} & C_{12} & C_{13} & 0 & 0 \\ C_{21} & C_{22} & C_{23} & 0 & 0 \\ C_{31} & C_{32} & C_{33} & 0 & 0 \\ 0 & 0 & 0 & C_{44} & 0 \\ 0 & 0 & 0 & 0 & C_{55} \end{bmatrix} \begin{bmatrix} -\zeta_1 \sin(\zeta_1 d/2) & \zeta_1 \cos(\zeta_1 d/2) & -i \xi \cos(\zeta_2 d/2) \\ -A_{11} & A_{12} & A_{13} \\ -\mu (\zeta_2^2 - \xi^2) \cos(\zeta_1 d/2) & -\mu (\zeta_2^2 - \xi^2) \sin(\zeta_1 d/2) & 2i \mu \xi \zeta_2 \cos(\zeta_2 d/2) \\ -2i \mu \xi \zeta_1 \sin(\zeta_1 d/2) & 2i \mu \xi \zeta_1 \cos(\zeta_1 d/2) & -A_{32} \\ -A_{51} & -A_{54} & -A_{53} \end{bmatrix} = 0$$

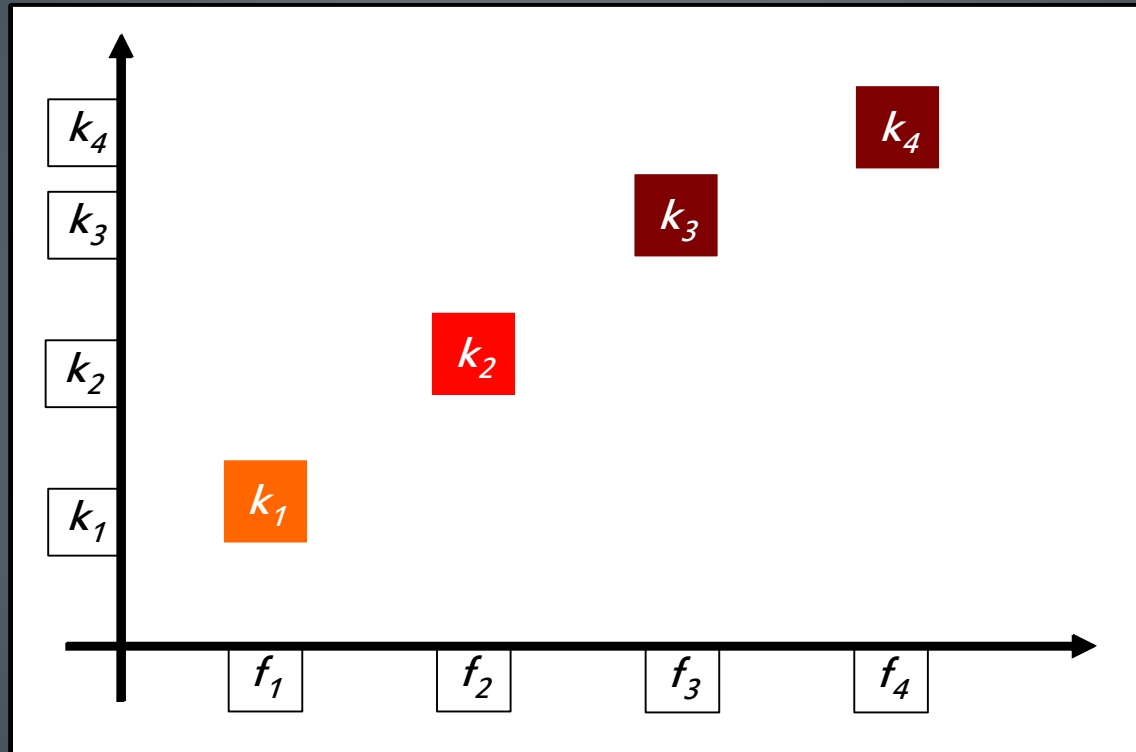
Next: Curve correlation

Slide 18

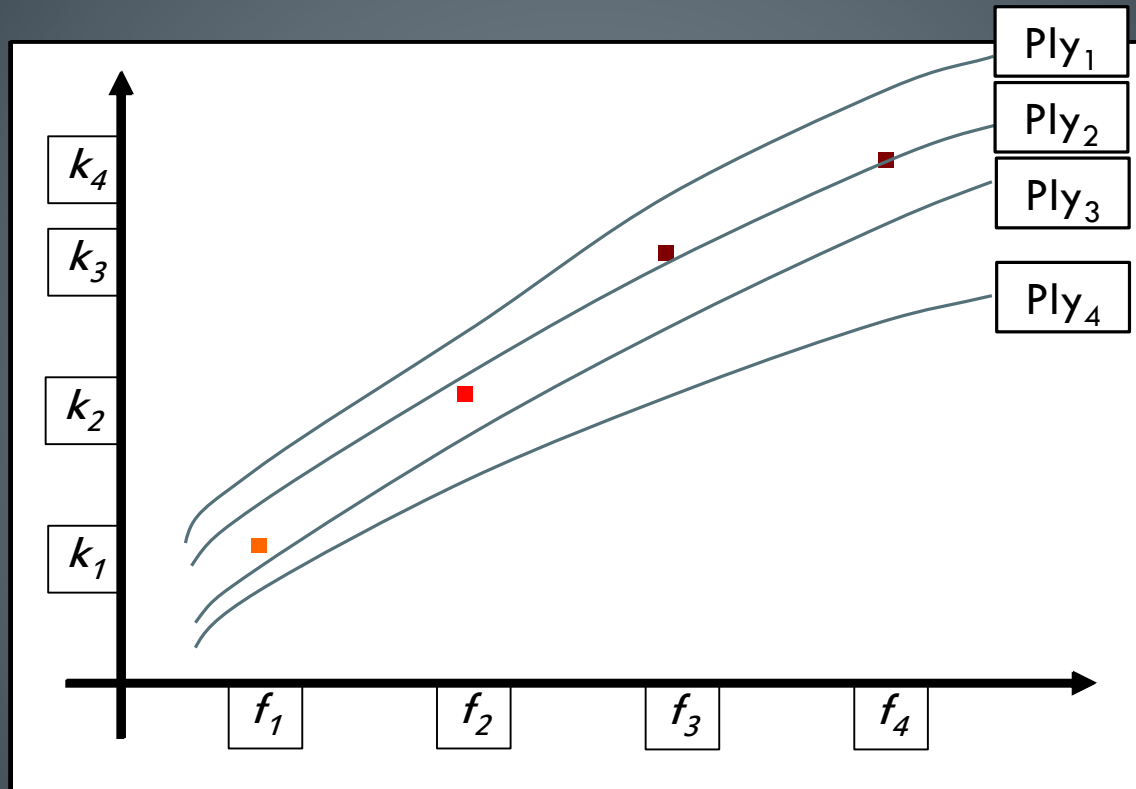
Multi-frequency wavenumber-ply correlation



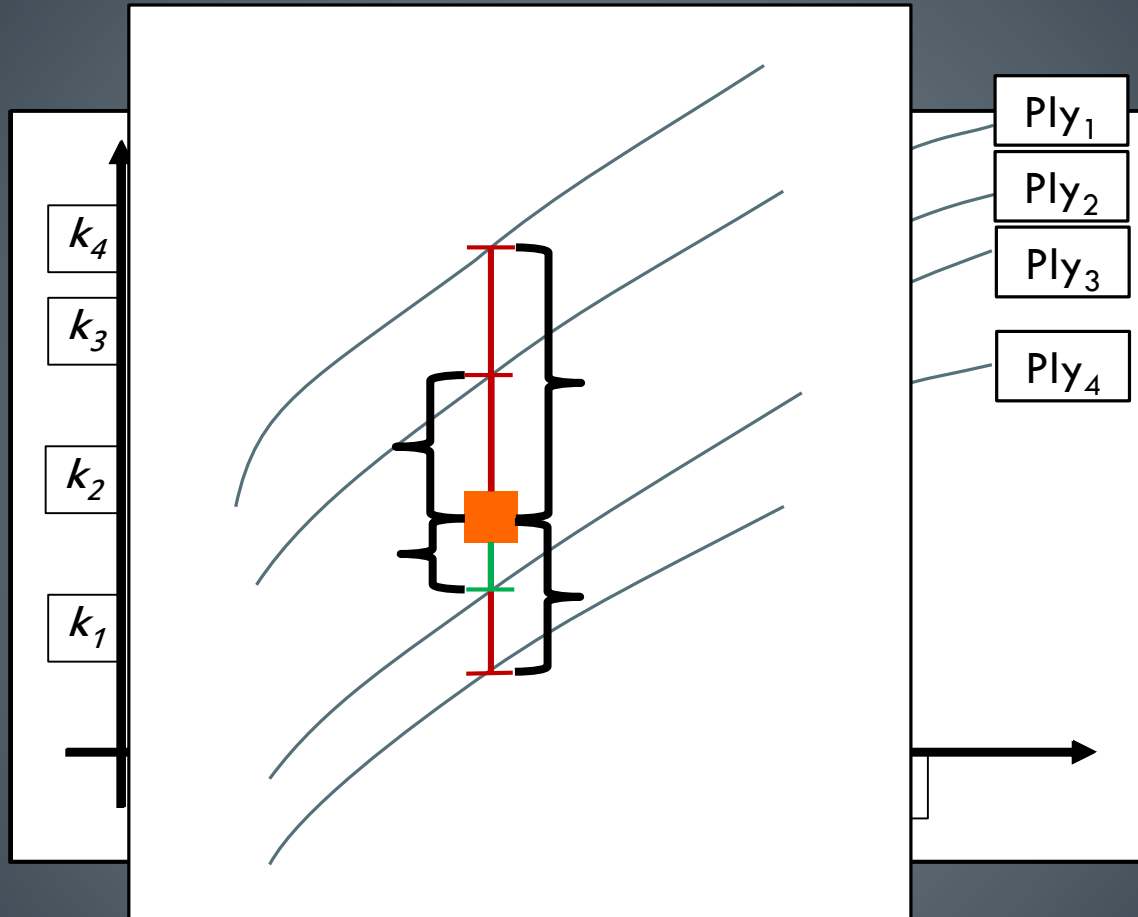
Multi-frequency wavenumber-ply correlation



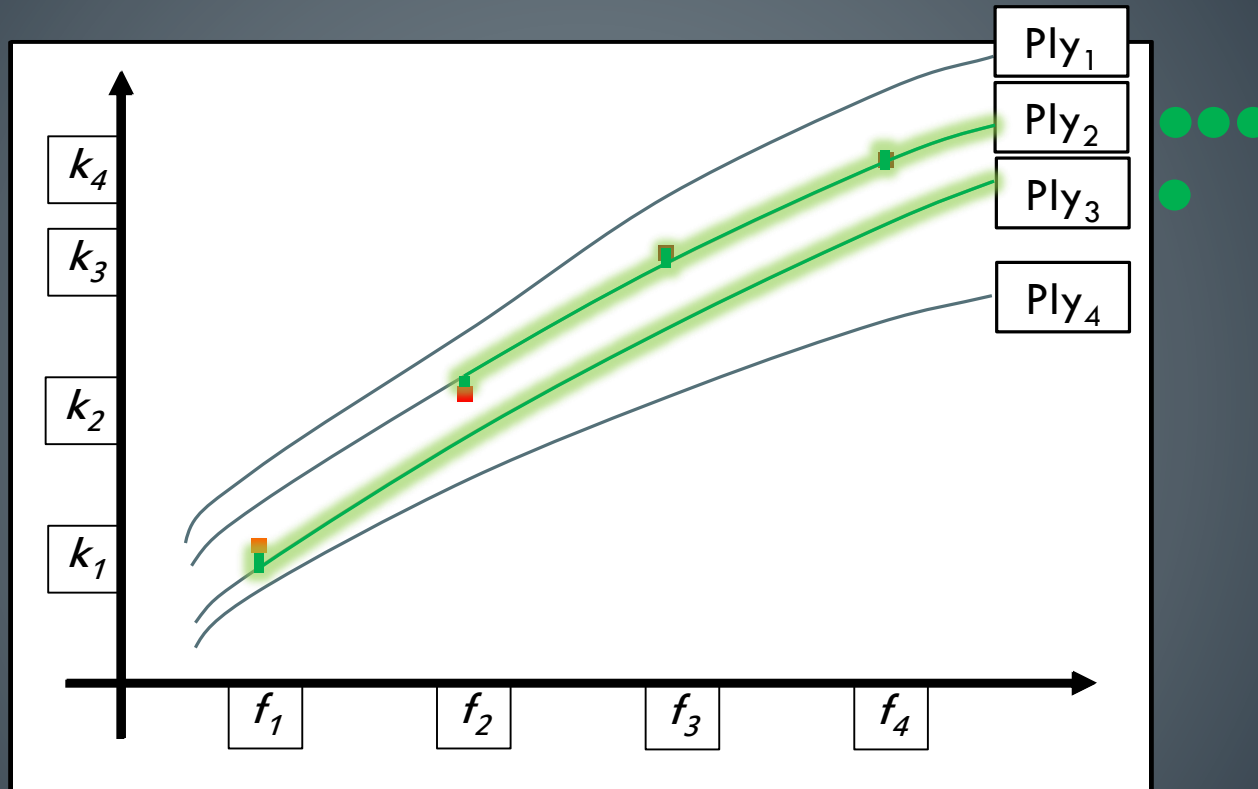
Multi-frequency wavenumber-ply correlation



Multi-frequency wavenumber-ply correlation

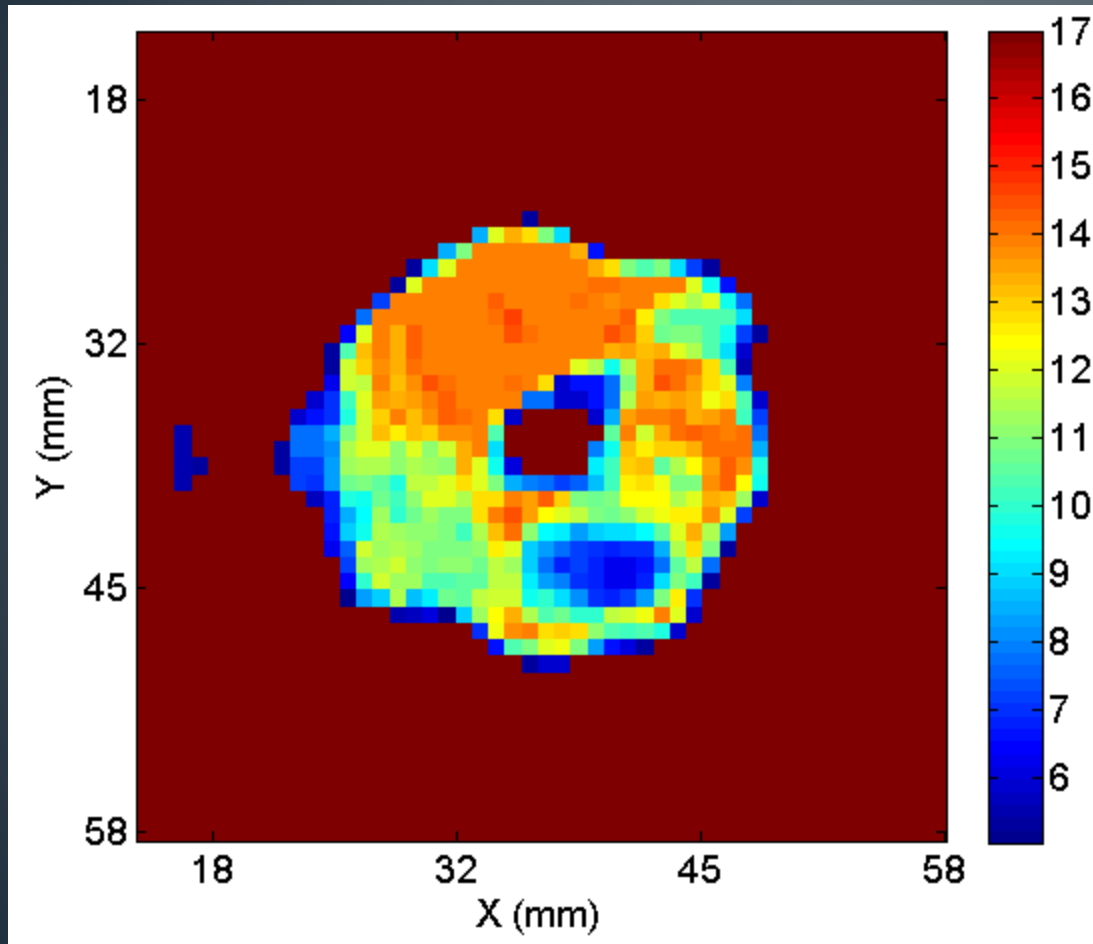


Multi-frequency wavenumber-ply correlation



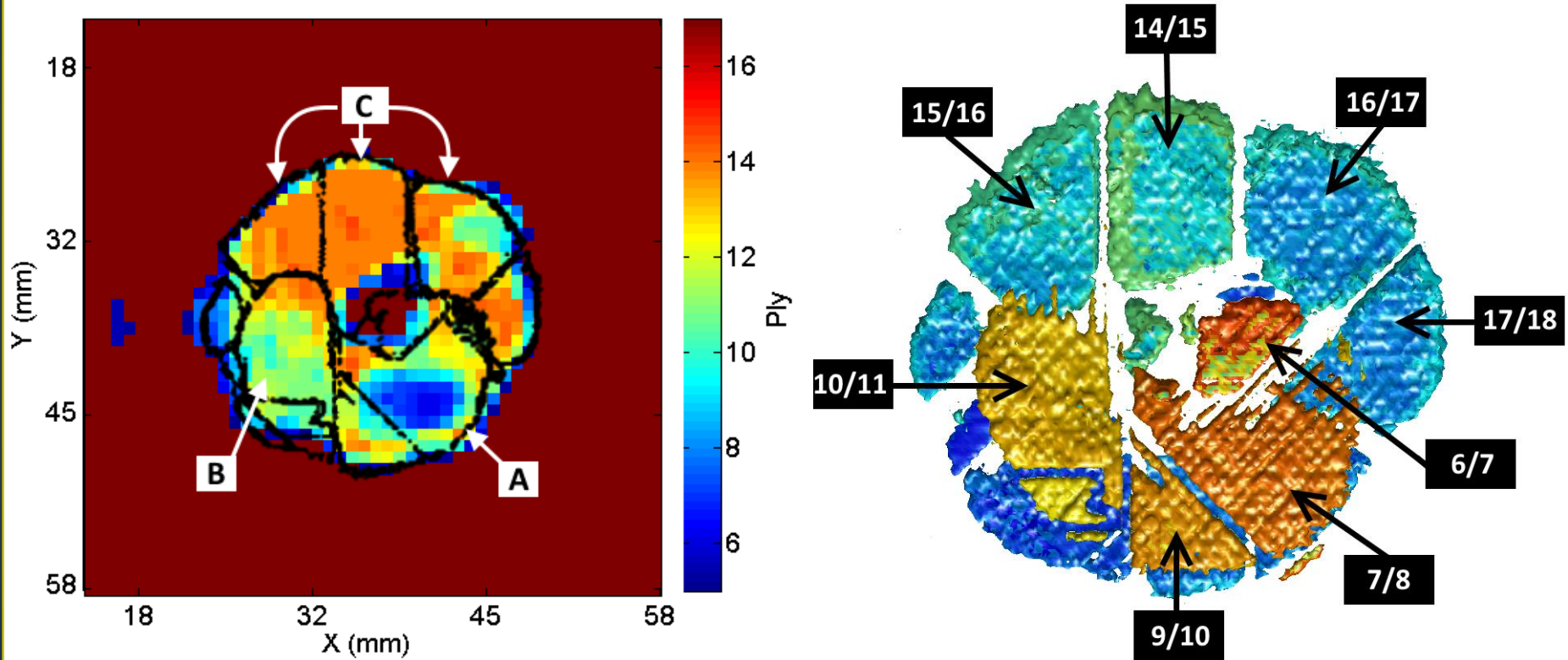
$$\text{Ply}(x, y) \approx \text{Ply}_2$$

Ply correlation results

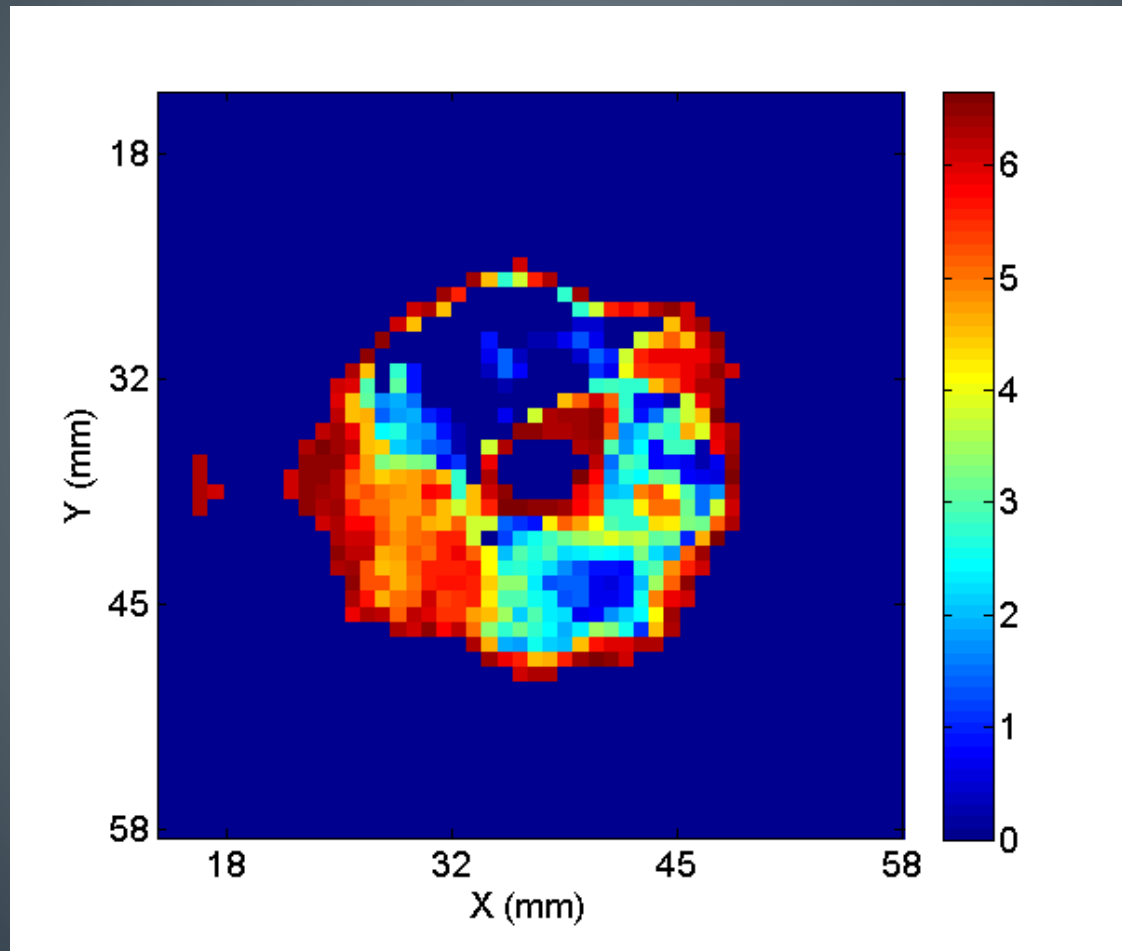


- Correlation frequency range: 300kHz-400kHz in 5kHz steps
- 10mm window
- 0.3mm spatial resolution
- 20MHz sampling rate

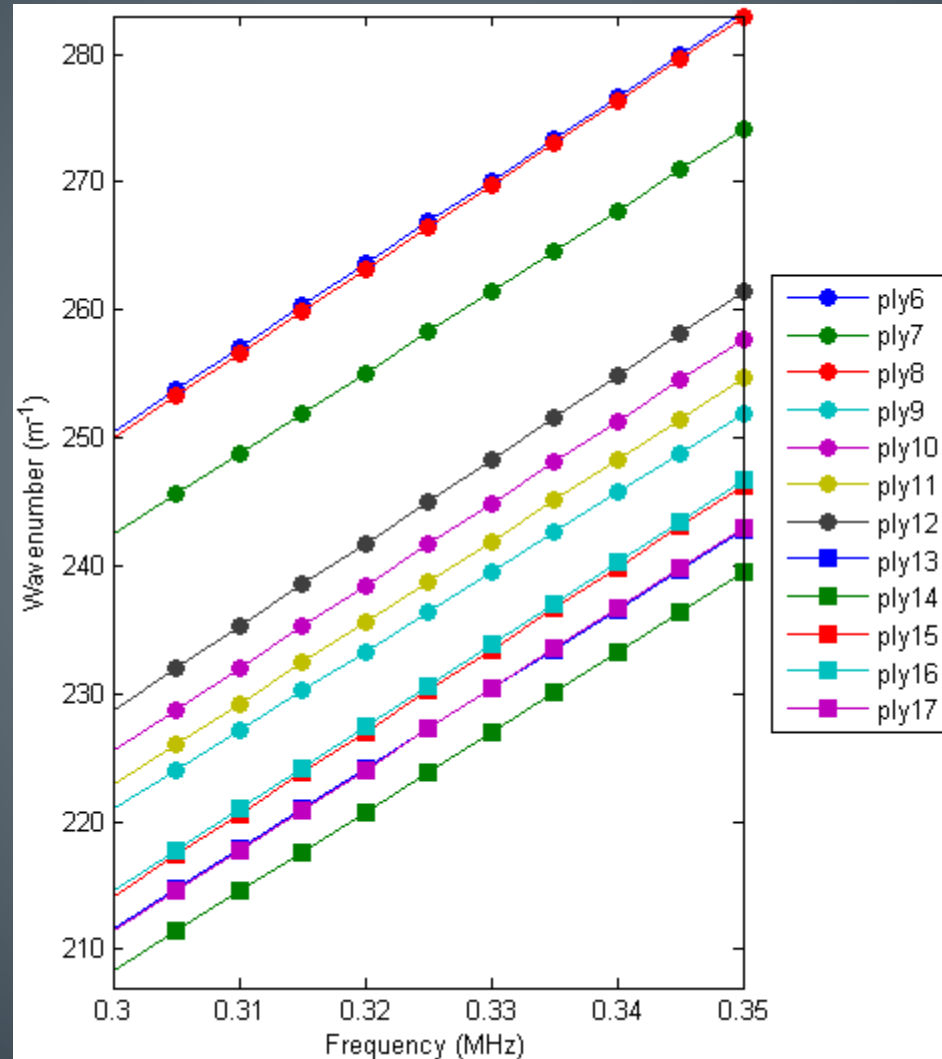
Ply correlation results



Sources of error: standard deviation



Sources of error: dispersion curves



Conclusions



- The local wavenumber technique is capable of very accurate determination of the shape and size of interlamina damage in composite panels, especially when considering multiple frequencies
- Using multi-frequency wavenumber-ply correlation can determine the depth location of damage in many instances, but struggles with deeper and smaller delaminations.
- Future research will be conducted to improve this methodology using wave domain filtering, better dispersion curve generation, and more robust correlation methods.

References



- I.M. Daniel, O. Ishai
Engineering Mechanics of Composite Materials (second Ed.)Oxford University Press, New York (2006)
- E. Madaras, C. Poe, J. Heyman, Combing fracture mechanics and ultrasonic NDE to predict the strength remaining in thick composites subjected to low-level impact, in: IEEE 1986 Ultrasonics Symposium, 1986, pp. 1051–1060, <http://dx.doi.org/10.1109/ULTSYM.1986.198898>.
- M. Richardson, M. Wisheart
Review of low-velocity impact properties of composite materials
Compos Part A: Appl Sci Manuf, 27 (12) (1996), pp. 1123–1131
- P. Johnston, C. Wright, J. Zalameda, J. Seebo, Ultrasonic monitoring of ply crack and delamination formation in composite tube under torsion load, in: Ultrasonics Symposium (IUS), 2010 IEEE, 2010, pp. 595–598, <http://dx.doi.org/10.1109/ULTSYM.2010.5935887>.
- B. Li, Y. Liu, K. Gong, Z. Li
Damage localization in composite laminates based on a quantitative expression of anisotropic wavefront
Smart Mater. Struct., 22 (6) (2013), p. 065005
- Z. Liu, F. Yu, R. Wei, C. He, B. Wu
Image fusion based on single-frequency guided wave mode signals for structural health monitoring in composite plates
Mater. Eval., 71 (2013), pp. 1434–1443
- J.E. Michaels, A.J. Dawson, T.E. Michaels, M. Ruzzene, Approaches to hybrid shm and nde of composite aerospace structures, in: SPIE Smart Structures and Materials+ Nondestructive Evaluation and Health Monitoring, International Society for Optics and Photonics, 2014, pp. 906427–906427.
- M.D. Rogge, C.A. Leckey
Characterization of impact damage in composite laminates using guided wavefield imaging and local wavenumber domain analysis
Ultrasonics, 53 (7) (2013), pp. 1217–1226
- J. Kilpatrick, A. Apostol, V. Markov, Design and applications of a high-speed Doppler imaging vibrometer, in: SPIE Optical Engineering+ Applications, International Society for Optics and Photonics, 2010, pp. 77910B–77910B.
- T.E. Michaels, J.E. Michaels, M. Ruzzene
Frequency–wavenumber domain analysis of guided wavefields
Ultrasonics, 51 (4) (2011), pp. 452–466
- Z. Tian, L. Yu, C. Leckey
Delamination detection and quantification on laminated composite structures with lamb waves and wavenumber analysis
J. Intell. Mater. Syst. Struct. (2014) 1045389X14557506
- C.A. Leckey, M.D. Rogge, C.A. Miller, M.K. Hinders
Multiple-mode lamb wave scattering simulations using 3d elastodynamic finite integration technique
Ultrasonics, 52 (2) (2012), pp. 193–207
- C.A. Leckey, M.D. Rogge, F.R. Parker
Guided waves in anisotropic and quasi-isotropic aerospace composites: three-dimensional simulation and experiment
Ultrasonics, 54 (1) (2014), pp. 385–394 <http://dx.doi.org/10.1016/j.ultras.2013.05.007>
- H. Sohn, D. Dutta, H. Yang, M. Park, M. DeSimio, S. Olson, E. Swensen
Delamination detection in composites through guided wave field image processing
Compos. Sci. Technol., 71 (2011), pp. 1250–1256

References



C.A.C. Leckey, J. Seebo

Guided wave energy trapping to detect hidden multilayer delamination damage

Rev. Progress Quant. Nondestruct. Eval., 34 (1650) (2015), pp. 1162–1169

E.B. Flynn, S.Y. Chong, G.J. Jarmer, J.-R. Lee

Structural imaging through local wavenumber estimation of guided waves

NDT & E Int., 59 (2013), pp. 1–10

O. Mesnil, C.A.C. Leckey, M. Ruzzene, Instantaneous and local wavenumber estimations for damage quantification in composites, Struct. Health Monitoring <http://dx.doi.org/10.1177/1475921714560073>.

J.E. Michaels, S.J. Lee, A.J. Croxford, P.D. Wilcox

Chirp excitation of ultrasonic guided waves

Ultrasonics, 53 (1) (2013), pp. 265–270 <http://dx.doi.org/10.1016/j.ultras.2012.06.010>

V. Herb, G. Couégnat, E. Martin

Damage assessment of thin SiC/SiC composite plates subjected to quasi-static indentation loading

Compos. Part A: Appl. Sci. Manuf., 41 (11) (2010), pp. 1677–1685

G. Williams, R. Trask, I. Bond

A self-healing carbon fibre reinforced polymer for aerospace applications

Compos. Part A: Appl. Sci. Manuf., 38 (6) (2007), pp. 1525–1532

V.V. Bolotin

Delaminations in composite structures: its origin, buckling, growth and stability

Compos. Part B: Eng., 27 (2) (1996), pp. 129–145 [http://dx.doi.org/10.1016/1359-8368\(95\)00035-6](http://dx.doi.org/10.1016/1359-8368(95)00035-6)

G. Clark

Modelling of impact damage in composite laminates

Composites, 20 (3) (1989), pp. 209–214 [http://dx.doi.org/10.1016/0010-4361\(89\)90335-2](http://dx.doi.org/10.1016/0010-4361(89)90335-2)

B. Pavlakovic, M. Lowe, D. Alleyne, P. Cawley

Disperse: a general purpose program for creating dispersion curves

Review of Progress in Quantitative Nondestructive Evaluation, Springer (1997), pp. 185–192